ELEMENTA
Science of the Anthropocene

Fisher, JA and Nelson, PF. 2020. Atmospheric mercury in Australia: Recent findings and future research needs. *Elem Sci Anth*, 8: 1. DOI: https://doi.org/10.1525/elementa.2020.070

REVIEW

Atmospheric mercury in Australia: Recent findings and future research needs

Jenny A. Fisher[1,*] and Peter F. Nelson[2]

Mercury is a toxic bioaccumulative pollutant, with the atmosphere being the primary pathway for global distribution. Although atmospheric mercury cycling has been extensively monitored and modeled across the Northern Hemisphere, there has long been a dearth of mercury data for the Southern Hemisphere. Recent efforts in Australia are helping to fill this gap, with new observational records that span environments ranging from cool temperate to warm tropical climates and near-source to background conditions. Here, we review recent research on atmospheric mercury in Australia, highlighting new observational constraints on atmospheric concentrations, emissions, and deposition and, where possible, comparing these to model estimates. We also provide our best estimate of the current Australian atmospheric mercury budget. Ambient mercury observations collected to date show unique features not captured at other observing sites across the Southern Hemisphere, including very low concentrations at inland sites and a monsoon season drawdown in the tropical north. Previously compiled estimates of Australian anthropogenic mercury emissions differ substantially due to both methodological differences (e.g., assumptions about mercury control technology in coal-fired power plants) and recent closures of major Australian mercury sources, and none are appropriate for modern-day Australia. For mercury emissions from biomass burning, new measurements from Australian smoke plumes show emission factors for both savanna and temperate forest fires are significantly lower than measured elsewhere in the world, and prior estimates based on non-Australian data are likely too high. Although significant uncertainties remain, our analysis suggests that emissions from terrestrial sources (both newly released and legacy) significantly exceed those from anthropogenic sources. However, recent bidirectional air-surface flux observations suggest this source is likely balanced by deposition and surface uptake at local scales. Throughout, we highlight lingering uncertainties and identify critical future research needs for understanding Australian atmospheric mercury and its role in Southern Hemisphere mercury cycling.

Keywords: Mercury, Australia, Emissions, Biomass burning, Air-surface exchange, Deposition

1. Introduction

Mercury is a naturally occurring metal that cycles between the atmosphere, ocean, and terrestrial reservoirs and is toxic to humans and wildlife when converted to its organic methylated form (Selin, 2009). Over millennia, anthropogenic emissions of mercury have enhanced the transfer of mercury from the stable rock reservoir to the atmosphere, a process that has accelerated since the Industrial Revolution (Amos et al., 2013). With an atmospheric lifetime of several months, mercury in the atmosphere is transported on hemispheric scales (Corbitt et al., 2011). In recognition of the global nature of the mercury problem, the United Nations Environment Programme Minamata Convention on Mercury entered into force in 2017. The Convention includes provisions to reduce emissions of mercury to the atmosphere with the overarching goal of reducing mercury in the environment. A key challenge now is evaluating the effectiveness of actions undertaken in response to the Convention, which relies on underlying knowledge of mercury's sources, distribution, transformation and fate.

In Australia, establishing this baseline has been a challenge due to a historic sparsity of observations. As of 2019, Australia was the only continent without a single long-term (>10-year) air monitoring site (Arctic Monitoring and Assessment Programme [AMAP]/United Nations Environment Programme [UNEP], 2019). Although countries in North America and Europe have developed extensive atmospheric mercury monitoring networks over the past several decades, the first ongoing atmospheric measurement site in Australia was not established until 2011. Since then, however, efforts have been made to begin closing this data gap. As shown in **Figure 1**, a number

[1] Centre for Atmospheric Chemistry, School of Earth, Atmospheric and Life Sciences, University of Wollongong, Wollongong, New South Wales, Australia

[2] Department of Earth and Environmental Sciences, Macquarie University, Sydney, New South Wales, Australia

* Corresponding author:
Email: jennyf@uow.edu.au

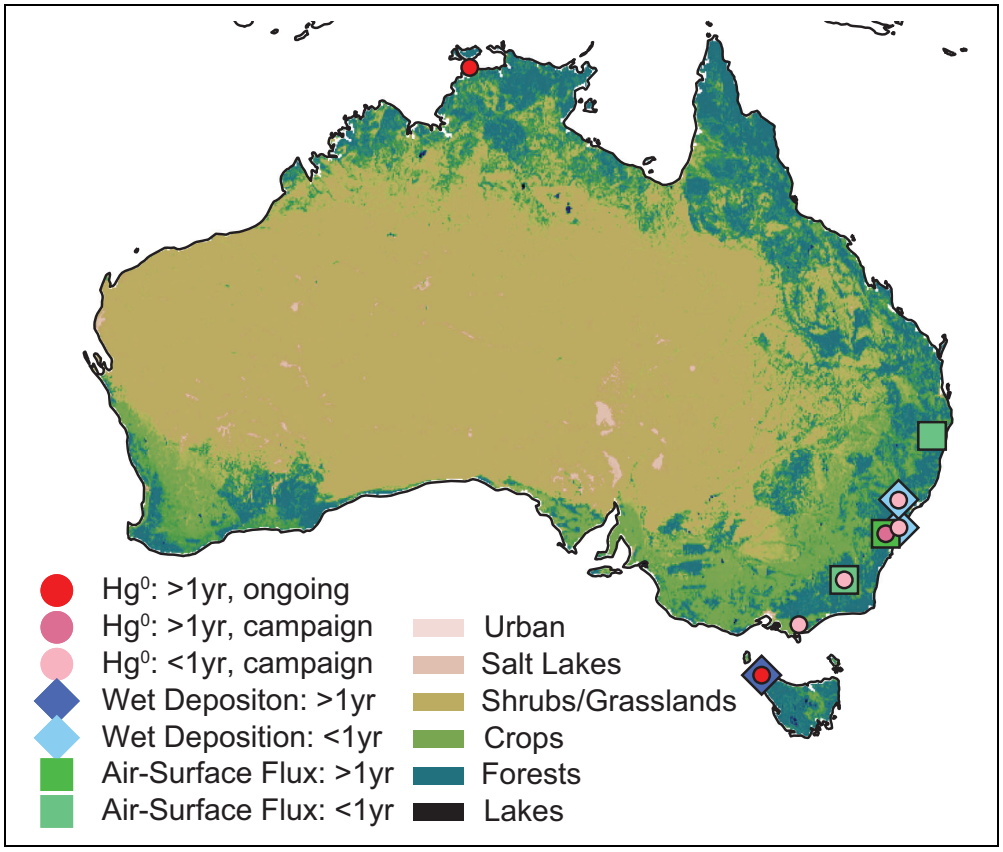

Figure 1. Locations of measurements relevant to Australian atmospheric mercury. The map shows the locations of measurements relevant to Australian atmospheric mercury, including elemental mercury concentrations (circles), mercury wet deposition fluxes (diamonds), and mercury air-surface exchange fluxes (squares), shown separately for long-term (>1 year, dark colors) and short-term (<1 year, light colors) data sets. For elemental mercury, sites with ongoing measurements are shown in red. The map background shows land cover from the Geoscience Australia Dynamic Land Cover Dataset (Lymburner et al., 2015). DOI: https://doi.org/10.1525/elementa.2020.070.f1

of new measurements from both ongoing monitoring stations and short-term field campaigns are beginning to shed light on the Australian mercury cycle.

With diverse environments spanning from the monsoonal tropics to the Southern Ocean, vast inland deserts, unique flora, and a small population concentrated in a few urban centers, the Australian continent is unlike other parts of the world where mercury cycling has been extensively studied. Australia also offers unique opportunities to study the biogeochemistry of mercury. Initial inventory estimates discussed here suggest that emissions of newly released and legacy terrestrial mercury significantly exceed those from anthropogenic sources. The population distribution, which is largely concentrated on the coast, results in opportunities to investigate land-based mercury cycling in the effective absence of confounding local industrial or domestic sources.

Australian-specific understanding of mercury's sources and sinks is needed. This review presents our current understanding of Australian atmospheric mercury. Section 2 describes mercury concentrations and distributions in the Australian atmosphere. Section 3 details sources of mercury to the atmosphere and how these have changed in recent years. Section 4 addresses mercury deposition to the Australian surface. Throughout these sections, we highlight new observations collected over the past decade, compare these to model estimates, and identify the remaining research gaps. Finally, Section 5 concludes the review with our best estimate of the current Australian atmospheric mercury budget and our recommendations for addressing the most critical future research needs.

2. Mercury in the Australian atmosphere

2.1. Elemental mercury

Measurements of ambient elemental mercury (Hg^0) suggest atmospheric concentrations in Australia fall at or below the approximately 1 ng m^{-3} Southern Hemisphere background. Long-term (>1 year) Australian measurements are limited to three remote sites (see **Figure 1**). Slemr et al. (2015) first reported Australian atmospheric elemental mercury concentrations of only 0.85 ng m^{-3} based on measurements at Cape Grim in northwest Tasmania from 2011 to 2013. However, subsequent analysis determined continuous exposure to sea salt at the exposed site was passivating the gold trap in the Cape Grim Tekran 2357A instrument, reducing the mercury capture efficiency. Data collected after updating the measurement protocol to address the issue show 2013–2016 ambient concentrations that are slightly higher at 0.90 $\pm$ 0.10 ng m^{-3} (Page, 2018) but still roughly 10% lower than

those measured at other Southern Hemisphere midlatitude sites (Slemr et al., 2015). It is unclear whether this difference represents real geographic variability or measurement uncertainty, as systematic uncertainties in Tekran measurements are expected to be of order 10% and can be up to 20% in extreme circumstances (Slemr et al., 2015). In addition, passive samplers deployed at Cape Grim in 2015–2016 found higher mean mercury concentrations of 1.03 $\pm$ 0.02 ng m^{-3}, with a mean normalized difference of 17 $\pm$ 2% relative to simultaneous Tekran measurements (McLagan et al., 2018). Although the authors attribute the difference to uncertainty in the passive samplers (which is high at Cape Grim due to corrections needed for the strong westerly winds at the site), it is also possible that some contribution comes from low bias in the Cape Grim Tekran observations.

The only other extant multiyear mercury observations come from Gunn Point in Australia's monsoonal north. Howard et al. (2017) report 2014–2016 average elemental mercury concentrations at Gunn Point of 0.95 $\pm$ 0.12 ng m^{-3} but with a strong seasonal signature. Wet season mean concentrations of 0.90 $\pm$ 0.10 ng m^{-3} are lower than dry season means of 0.97 $\pm$ 0.13 ng m^{-3}. The observations show a gradual decline in atmospheric mercury over the wet season attributed to wet scavenging in monsoonal precipitation combined with suppressed reemission from saturated soils (Howard et al., 2017). The observations also show occasional incursions of Northern Hemisphere air during the wet season associated with movement of the Intertropical Convergence Zone. Observed mercury is 20% higher during these events than during the rest of the wet season (Howard et al., 2017).

Differences between Cape Grim and Gunn Point have been used to suggest the existence of a latitudinal gradient across Australia (Howard et al., 2017); however, these differences fall within the experimental uncertainties for the Tekran measurement (Slemr et al., 2015) and so are difficult to confirm. More striking is the difference between coastal and inland sites. New measurements at a rural inland site approximately 50 km from the coast in southeast Australia show surprisingly low elemental mercury concentrations of 0.68 $\pm$ 0.22 ng m^{-3} over a 14-month period, falling to 0.43 $\pm$ 0.08 ng m^{-3} in winter (MacSween et al., 2020). Similarly, low values of 0.59 $\pm$ 0.10 ng m^{-3} were measured at an alpine site in summer (Howard and Edwards, 2018). These low values may reflect the largely oceanic source of background mercury in the Southern Hemisphere (Horowitz et al., 2017), coupled with substantial deposition taking place during air mass transport.

To date, limited efforts have been made to use these new long-term observational data sets to constrain atmospheric mercury models. Analysis of global model capability based on two other sites in the Southern Hemisphere midlatitudes has shown poor model ability to represent observed concentrations and seasonality (Song et al., 2015; Horowitz et al., 2017). Current state-of-the-science global mercury models show average Australia-wide elemental mercury concentrations of 1.0 $\pm$ 0.10 ng m^{-3} with little spatial variability across the continent (Travnikov et al., 2017; AMAP/UNEP, 2019). Adding the recent Australian data to future model validation efforts will provide improved constraints on the relevant drivers of variability and the implications for improving model performance.

As expected, elemental mercury concentrations are higher near known emission sources, although measurements in these regions are limited to short-term campaigns. In suburban northwest Sydney, background values of approximately 1 ng m^{-3} were seen during a 10-day period in summer, with peak values up to 2 ng m^{-3} (Nelson et al., 2009). In the Latrobe Valley, a major coal-fired power-producing region of Australia, observed concentrations averaged 1.5 ng m^{-3} over a 2-month (May–June) period (Schofield et al., n.d.). Regional model simulations for the Latrobe Valley have successfully simulated both mean concentrations (Emmerson et al., 2015; Schofield et al., n.d.) and a significant fraction of the variability (Schofield et al., n.d.). With only short data sets currently available, long-term observations are needed to contextualize these data.

Substantial long-term continuous measurements have also been made at sites in the Hunter Valley approximately 200 km north of Sydney. The Hunter Valley is the location of potentially significant sources of mercury from coal-fired power generation (Bayswater and Liddell power stations, 4640 MW total capacity) and large-scale open-cut and underground coal mining. Mercury measurements at these sites have been undertaken for more than 10 years, but the data have not yet been extensively analyzed. However, a preliminary analysis was performed on more than 12 months of sampling (Morrison et al., 2015). Results from this analysis confirmed that mean annual ambient total gaseous mercury levels were 0.86 ng m^{-3}, but ranged from 0.19 to 2.48 ng m^{-3}. Simultaneous measurements of sulfur dioxide (SO_2) showed no convincing relationship between mercury and SO_2, a proxy for power station plumes. Although SO_2 variations were consistent with plumes from the power station mixing down to ground level, mercury concentrations usually increased overnight or in the early morning. The latter suggests the mercury comes from ground-based sources and accumulates at the surface overnight under the low nocturnal boundary layer.

2.2. Reactive mercury

Measurements of reactive mercury are scarce even at the global scale (AMAP/UNEP, 2019); in Australia, they are virtually nonexistent. At the Hunter Valley site, gaseous oxidized mercury (Hg^{II}) measurements made over 6 months spanning austral spring to autumn (November–April) showed mean concentrations of 11.28 pg m^{-3} with occasional high values of up to 164.21 pg m^{-3} (Morrison et al., 2015). The only other published reactive mercury measurements are from a 1-month campaign that took place at Gunn Point in June 2014 (during the dry season). These data show mean Hg^{II} concentrations of 11 $\pm$ 5 pg m^{-3} and particulate-bound mercury (Hg^{P}) of 6 $\pm$ 3 pg m^{-3}; combined Hg^{II} and Hg^{P} comprised up to 3.4% of the total observed atmospheric mercury (Mallet et al., 2017). In the absence of observational constraints, models show large variability in simulating reactive

Table 1. Australian anthropogenic emission totals (top line) and speciation (bottom line, italics). DOI: https://doi.org/10.1525/elementa.2020.070.t1

Inventory	Year	Hg^0 (t yr^{-1})	Hg^{II} (t yr^{-1})	Hg^P (t yr^{-1})	Total Hg (t yr^{-1})
Nelson et al. (2012)	2006	11.5	2.5	1.0	15.0
		77%	*17%*	*7%*	
AMAP/UNEP[a] (2013)	2010	15.4	3.8	1.2	20.4
		75%	*19%*	*6%*	
WHET[b] (2016)	2010	21.9	3.9	1.3	27.1
		81%	*14%*	*5%*	
EDGARv4.tox2 S1[c] (2018)	2012	12.2	5.1	1.3	18.6
		66%	*27%*	*7%*	
EDGARv4.tox2 S3[d] (2018)	2012	13.3	4.9	0.3	18.6
		72%	*26%*	*2%*	
AMAP/UNEP[e] (2019)	2015	n/a	n/a	n/a	7.7

[a]Arctic Monitoring and Assessment Programme/United Nations Environment Programme inventory developed for the Global Mercury Assessment 2013 (AMAP/UNEP, 2013).

[b]World Hg Emission Trends (Zhang et al., 2016).

[c]Emission Database for Global Atmospheric Research version 4.tox2, Scenario 1 (Muntean et al., 2018). The contribution from agricultural waste burning (total Hg: 2.1 t yr^{-1}) has been subtracted as it is not included in the other anthropogenic inventories.

[d]Same as note (c) above but for Scenario 3 (Muntean et al., 2018). Sectoral contributions are not provided for S3, so to subtract the contribution from agricultural waste burning, we have assumed the same speciation for this sector as provided in S1 (20% Hg^0, 60% Hg^{II}, 20% Hg^P).

[e]Arctic Monitoring and Assessment Programme/United Nations Environment Programme inventory developed for the Global Mercury Assessment 2018 (AMAP/UNEP, 2019). Speciated information for Australia is not available.

mercury. Over Australia, global models show background concentrations could be anywhere from 5 to 40 pg m^{-3}, with inter-model differences largely dependent on model chemical mechanisms and removal process parameterizations (Travnikov et al., 2017).

2.3. Summary and recommendations

The last decade has seen the establishment of the first long-term mercury observation stations in Australia at Cape Grim in the south (since 2011) and Gunn Point in the tropical north (since 2014). Measurements from these coastal sites show background elemental mercury of 0.9–1.0 ng m^{-3}, somewhat lower than that seen at other Southern Hemisphere sites but within the range of experimental uncertainty. Combining these data with measurements from a 14-month campaign in inland southeast Australia suggests a potential gradient in elemental mercury, with significantly lower concentrations observed inland than at coastal sites. Global models have yet to exploit these new data for validation and development purposes despite known deficiencies in simulating mercury variability in the Southern Hemisphere.

The ambient mercury observations collected to date in Australia show unique features not captured at other observing sites across the Southern Hemisphere (e.g., the monsoonal drawdown in the tropical north and the very low concentrations at inland sites). Maintaining and expanding this network (including with the addition of reactive mercury measurements) will be critical for constraining Australian mercury cycling and for monitoring the effectiveness of Southern Hemisphere emission reductions associated with the Minamata Convention.

3. Emissions of mercury to the Australian atmosphere

The most comprehensive accounting of atmospheric mercury emissions in Australia was compiled by Nelson et al. (2012) using 2006 data. The authors found that anthropogenic sources comprised only 7% of total Australian mercury emissions with the remainder attributed to fires (21%) and vegetation and soil sources (72%). Here we summarize what is known about each of these sources, including sectoral contributions, comparisons to other estimates, uncertainties, and recent changes that are likely to have a significant impact on estimated Australian mercury emissions.

3.1. Anthropogenic emissions

Table 1 compares the Australia-specific emissions from Nelson et al. (2012) to the Australian contribution included in global inventories. Most global inventories do not publish country-level totals for Australia, so we calculate the values shown in **Table 1** directly from the emission data files. The exception is the AMAP/UNEP

Table 2. Major sectoral contributions to Australian anthropogenic mercury emissions.[a] DOI: https://doi.org/10.1525/elementa.2020.070.t2

Inventory	Fossil Fuel Combustion[c] ($t\ yr^{-1}$)	Gold Production[d] ($t\ yr^{-1}$)	Other Metals[e] ($t\ yr^{-1}$)	Intentional Use and Waste[f] ($t\ yr^{-1}$)	Other Industry[g] ($t\ yr^{-1}$)
Nelson et al. (2012)	2.4	7.7	3.0	1.4	0.9
AMAP/UNEP (2013)	3.4	12.2	4.4	0.7	0.7
WHET[b] (2016)	13.9	5.6	2.1	5.2	0.2
EDGARv4.tox2 (2018)	8.8	6.3	2.9	0.05 [h]	0.5
AMAP/UNEP (2019)	3.1	1.8	0.9	0.9	0.8

[a]For inventory names and references, see **Table 1**.

[b]Sector-specific estimates are not available at country level in WHET, so the Australian sectoral contributions have been estimated here by scaling the Oceania totals (including Australia, New Zealand, Papua New Guinea, and Pacific Islands) by the Australia-to-Oceania ratio found in the total emissions (0.81).

[c]Based on the following categories: coal combustion in power plants and combustion of oil in Nelson et al.; stationary combustion—power plants, industry, and domestic/residential/other (coal, oil, gas) in AMAP/UNEP; coal and oil in WHET; and power generation, industry (combustion), and residential (combustion) in EDGARv4.tox2.

[d]Based on the following categories: gold smelting and gold mining in Nelson et al.; large-scale gold production in AMAP/UNEP; gold, large-scale and gold, artisanal in WHET; and gold production (large-scale and small-scale gold production, mercury production, and chlor-alkali mercury cell tech) in EDGARv4.tox2. Note that EDGARv4.tox2 includes mercury production and chlor-alkali industry in this category, whereas these are not included in the other inventories.

[e]Based on the following categories: copper, zinc, lead, and silver smelting, alumina production from bauxite, primary ferrous metal production, production of recycled ferrous metals, and copper, zinc, lead, and silver mining in Nelson et al.; ferrous metal production (primary pig iron and steel, secondary steel), nonferrous metal production (primary copper/lead/zinc, primary aluminum, mercury production) in AMAP/UNEP; copper, zinc, lead, iron, and steel in WHET; and iron and steel and nonferrous: zinc, copper, and lead in EDGARv4.tox2.

[f]Based on the following categories: chlor-alkali production, biomedical waste incineration, electrical and electronic switches, light sources, measuring equipment, laboratory equipment, dental amalgam, batteries, and crematoria/cemeteries in Nelson et al.; cremation emissions, waste (other waste), waste incineration (controlled burning) in AMAP/UNEP; waste, caustic soda, and additional air from Horowitz et al. (2014) in WHET; and solid waste incineration in EDGARv4.tox2.

[g]Based on the following categories: coke production, cement and lime production, oil refining pulp and paper production in Nelson et al.; cement production (raw materials and fuel, excluding coal), oil refining in AMAP/UNEP; cement in WHET; and cement, transformation industry, and refineries (combustion) in EDGARv4.tox2.

[h]Solid waste incineration only; other forms of waste and cremation emissions are not included in EDGARv4.tox2.

(2019) inventory, for which Australian totals are provided directly in the accompanying technical document.

Table 1 shows that the speciation of mercury emissions is similar between the different inventories, with most mercury emitted as Hg^0 (66%–81%), followed by reactive gaseous Hg^{II} (14%–27%) and then particulate-bound Hg^P (2%–7%). However, estimates of total mercury emission vary by more than a factor of three. To better understand the differences between inventories, **Table 2** shows sectoral contributions to total Australian mercury emissions. These are discussed further in the following subsections (with the exception of "Other Industry," comprising cement production and oil refining, which provides a small contribution to all inventories).

3.1.1. Fossil fuel combustion

A significant source of variability between the inventories comes from stationary combustion (mainly coal) at power plants, with estimates ranging from 2.4 t yr^{-1} (Nelson et al., 2012) to 13.9 t yr^{-1} (WHET) as shown in **Table 2**. The range likely reflects differing assumptions about mercury capture in pollution control devices in Australian power plants. Although Australian power plants are not equipped with the flue-gas desulfurization technology common elsewhere in the world (Dave et al., 2011; Sinclair and Schneider, 2019), most are equipped with either cold side electrostatic precipitation and/or fabric filtration (Nelson et al., 2009). For the black (bituminous) coal burned at power stations in Queensland and New South Wales, fabric filtration (used for 57% of total installed black coal capacity) is thought to reduce emissions by 83% (Nelson et al., 2009) and electrostatic precipitation (installed for 43% of black coal capacity) by 46.5%. For brown coal, Nelson et al. (2012) suggest that up to 50% of the mercury liberated from brown coal may be captured by the existing pollution control technology.

Treatment of these mercury capture technologies in emission estimates has historically been a source of inaccuracy in global inventories. For example, Nelson et al. (2012) compared their inventory (with detailed local

pollution control estimates) to an earlier version of the AMAP/UNEP inventory (AMAP/UNEP, 2008), which assumed no mercury capture at Australian power plants, leading to stationary combustion emissions of 17.7 t yr^{-1}. The 2013 version of the inventory was updated to incorporate mercury capture at all Australian power plants following Nelson et al. (2009), resulting in a factor of 5 decrease in estimated power plant mercury emissions to 3.4 t yr^{-1}, more consistent with the low values estimated by Nelson et al. (2012).

We expect that similar assumptions explain the very high combustion emissions in the WHET inventory of Zhang et al. (2016). WHET is based largely on an earlier inventory developed by Streets et al. (2011), modified with artisanal-scale gold mining emissions from EDGARv4 (Muntean et al., 2014) and emissions from the use and disposal of commercial products from Horowitz et al. (2014). The Streets et al. (2011) inventory provides only aggregated regional values, with Australia included in the Oceania region, which is then spatially allocated in WHET using the distribution from the Global Emissions Initiative inventory (Zhang et al., 2016). We find here that Australia accounts for 81% of the Oceania totals in WHET. Applying this fraction to the original Streets et al. (2011) Oceania data used as input to WHET implies a contribution from stationary combustion of 13.9 t yr^{-1}, 6 times greater than the equivalent Australia-specific value from Nelson et al. (2012).

Details of the assumptions made by Streets et al. (2011) for emission control technology in Australian coal-fired power plants are not readily available. It seems likely, however, that mercury reduction technologies were not taken into account by Streets et al. (2011) (and, consequently, by Zhang et al., 2016), leading WHET to significantly overestimate mercury emissions from coal combustion. In fact, updated estimates provided by Streets et al. (2019) decrease the Oceania fossil fuel emissions by a factor of 2.5 (from 17.3 to 6.9 t yr^{-1}). Again, assuming Australia accounts for 81% of this total, this would reduce the WHET fossil fuel estimate to 5.6 t yr^{-1}. This large change suggests that updates to the WHET emission inventory are urgently needed before these emissions can be used for Australia.

Stationary combustion emissions in EDGARv4tox2 are lower than those in WHET but significantly higher than those in Nelson et al. (2012) and AMAP/UNEP. This difference may again reflect assumptions about pollution control technologies, which are included in EDGARv4tox2 but with no details provided for Australian power plants. Muntean et al. (2014) note the application of "country-specific shares of existing control systems" (e.g., flue-gas desulfurization, electrostatic precipitation, fabric filtration), but the distribution of these in Australian power plants is not specified. Given the historical underestimate by global inventories of mercury capture in Australian power plants, it seems likely that the EDGARv4tox2 emissions similarly underestimate mercury capture and overestimate stationary combustion emissions.

Two other factors may also contribute to overestimates of coal mercury emissions in some of the global inventories. The first is the assumed coal mercury content. The Nelson et al. (2012) inventory is based on an extensive database of mercury content in Australian coals compiled by the Australian Commonwealth Scientific and Industrial Research Organization (Dale, 2003; Riley et al., 2005) and on mercury content in the coals actually burnt in the power stations (Attalla et al., 2004). These studies show average Australian black coal mercury contents of 0.04–0.05 mg kg^{-1} (range of 0.01–0.13 mg kg^{-1}). For comparison, coal mercury contents reported in AMAP/UNEP (2019) for other countries can be as high as 0.29 mg kg^{-1}, with a default global average of 0.15 mg kg^{-1}. Australian coals are generally low in sulfur, which usually implies they are also low in pyrite (FeS_2), and as mercury is strongly associated with pyrite in many coals, Australian coals have relatively low mercury content compared to those in other locations.

In addition, brown coals (including those used extensively in Australian power plants) typically have high moisture content (up to 50%; Nelson, 2007; AMAP/UNEP, 2019). This can lead to errors if emission factors are calculated simply by multiplying coal consumption (typically reported on an "as received" basis) by coal mercury content (typically reported on a dry, ash-free basis) without correcting for coal moisture content (AMAP/UNEP, 2013, 2019). Although the Nelson et al. (2012) and AMAP/UNEP (2013, 2019) inventories account for both the low coal mercury content of Australian coals and the high moisture content of brown coals, it is not clear whether either is accounted for by WHET or EDGARv4tox2.

Overall, we suggest that mercury emissions from Australian fossil fuel sources are better reflected by the low-end estimates of Nelson et al. (2012) and AMAP/UNEP (2013, 2019) and most likely fall in the range of 2.4–3.4 t yr^{-1}.

3.1.2. Gold production

Gold production is responsible for the largest share of Australian mercury emissions in the Nelson et al. (2012) and AMAP/UNEP (2013) inventories and the second largest share in the others, with an average contribution of approximately 7 t yr^{-1}. The largest outliers are the two versions of the AMAP/UNEP inventory, with the 2013 version suggesting a very large gold production source of 12.2 t yr^{-1} that dropped to only 1.8 t yr^{-1} in the 2019 version.

In the case of gold production estimates, both methodological differences and the year for which the estimates were made are relevant to understanding the differences between the inventories. Nelson et al. (2012) found that a single facility in Kalgoorlie, Western Australia, emitted 7.6 t yr^{-1} of mercury, accounting for 99% of their gold production estimate and nearly half of their estimated total anthropogenic emissions. This estimate came from Australia's National Pollutant Inventory (NPI), a national database to which point-source facilities self-report emissions of mercury and other pollutants (provided emissions exceed a mandated threshold, currently set at 5 kg yr^{-1} for mercury). Meanwhile, the significantly larger AMAP/UNEP (2013) estimate was based on U.S. Geological Survey data for mine production of gold, scaled using generic global assumptions about ore content (4 g

Au and 5.5 g Hg per tonne ore extracted) and the proportion of ore mercury released to air (4%). For comparison, an analysis of gold ore samples from Kalgoorlie found large variability in mercury content, with average values of only 0.6–1.7 g Hg per tonne ore (Environ, 2006). These differences in data sources and methodologies can explain the large differences between Nelson et al. (2012) and AMAP/UNEP (2013), with the Nelson et al. (2012) estimate considered more reliable as it is based on Australia-specific data.

The drastic decrease from AMAP/UNEP (2013) to AMAP/UNEP (2019) primarily reflects technology upgrades implemented between the two estimates at the gold production facility in Kalgoorlie. In 2015, the facility installed a new ultrafine grinding mill to replace the Gidji roaster that was responsible for 90% of the mercury emissions (Metseo Australia Limited, 2015). At the same time, the associated Fimiston processing plant was upgraded with a new carbon regeneration kiln fitted with mercury emission reduction technology (exhaust gas scrubber, regenerative thermal oxidizer, and sulfur impregnated carbon scrubber; Kalgoorlie Consolidated Gold Mines Pty Ltd and Ramboll Environ Australia Pty Ltd, 2015). **Figure 2** shows the change from 2004 to 2017 in mercury emissions from the Kalgoorlie facility, as reported to the NPI. Emissions have been separated into contributions from the Gidji roaster (dark blue) and Fimiston processing plant (light blue). The figure shows a long-term decrease in emitted mercury from 2004 to 2014, followed by a drop of 94% from 2014 to 2016 due to the Gidji closure.

According to the most recent NPI reports, since 2016, annual Australian mercury emissions associated with gold mining and processing have been less than 300 kg yr^{-1}. Assuming these data are accurate, even the low-end AMAP/UNEP (2019) estimate of 1.8 t yr^{-1} significantly overestimates this source. This analysis implies that none of the existing inventories can safely be used to model or analyze Australian mercury after 2015 without first modifying the gold production contribution.

3.1.3. Production of other metals

Mercury emissions associated with mining and processing nonferrous (copper, zinc, lead, silver, alumina) and ferrous (iron, steel) metals range from 0.9 to 4.4 t yr^{-1}. In all inventories, these emissions are dominated by nonferrous metals (90%–100%). Again, the two extremes come from the two AMAP/UNEP (2013, 2019) inventories, with the other inventories showing good agreement around 2–3 t yr^{-1}.

Methodological differences can largely explain the differences between the inventories. For example, as for gold, Nelson et al. (2012) use NPI-based estimates for metal production emissions, while AMAP/UNEP (2013, 2019) scale emissions based on mining activity and assumed emission factors. The difference between the two AMAP/UNEP (2013, 2019) inventories can be attributed to the updated treatment of Australian mercury emission factors in the 2019 release. The 2019 release includes Australia-specific base emission factors for copper, lead, zinc, and alumina production, whereas the 2013 release used

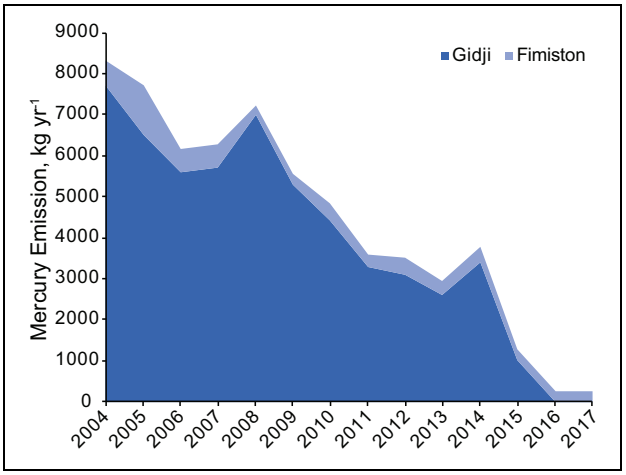

Figure 2. Trend in mercury emissions from gold processing in Kalgoorlie. 2004–2017 NPI-reported mercury emissions (kg yr^{-1}) from the Kalgoorlie Consolidated Gold Mines, showing contributions from the Gidji roaster (dark blue) and the Fimiston processing plant (light blue). Note that emissions are reported to NPI on a July–June financial year basis; in the figure, the year given on the *x*-axis corresponds to the year for the start of the reporting period (e.g., "2004" refers to July 2004–June 2005). DOI: https://doi.org/10.1525/elementa.2020.070.f2

generic emission factors for all of these sources except zinc. In addition, the 2019 release includes updated assumptions about the efficiency of air pollution control devices. As a result of both changes, mercury emissions associated with nonferrous metal production decreased by 81% from the 2013 to the 2019 release, even though changes in mining activity data between the two releases ranged from only a 15% decrease to a 5% increase.

Another potential confounding issue relates to details of the mineral processing and export arrangements in Australia. The emission estimates are often based on metal production data and emission factors. The amount of metal produced within the country is not necessarily a good basis for estimating emissions because mineral processing often involves production of an ore concentrate (by grinding and flotation processes) before high-temperature processing (by smelting or roasting) occurs. For many Australian metals, it is the ore and/or concentrate that is exported rather than the refined metal (Golev and Corder, 2016), and the processing emissions will occur elsewhere. This issue requires further investigation to more accurately estimate metal-related mercury emissions in Australia and likely in other countries as well.

3.1.4. Intentional use and waste

Mercury emissions from intentional use and waste derive from manufacturing processes that use mercury intentionally (e.g., chlor-alkali production using mercury cell technology), cremation, and breakage and disposal of products containing mercury (e.g., batteries, lights). The latter are highly uncertain and present a major source of discrepancies between the different inventories.

Table 3. Australian mercury emissions attributed to breakage and disposal of mercury-containing products.[a]
DOI: https://doi.org/10.1525/elementa.2020.070.t3

Inventory	Waste Emissions (kg yr^{-1})
Nelson et al. (2012)	887
AMAP/UNEP (2013)	617
WHET (2016)	5,124[b]
EDGARv4.tox2 (2018)	47
AMAP/UNEP (2019)	816

[a]Excludes intentional use in chlor-alkali plants and dental/cremation emissions. For inventory names and references, see **Table 1**.

[b]H Horowitz (personal communication).

The only inventory that includes mercury from intentional use in chlor-alkali plants is Nelson et al. (2012), which estimates 340 kg yr^{-1}, making this Australia's sixth largest mercury source in 2006. However, as the authors note, the only mercury cell chlor-alkali plant in Australia was demolished between 2004 and 2007, and the site remediated between 2013 and 2017 (Orica, 2014), with emissions dropping to only 8–9 kg yr^{-1} from 2007 to 2011 and to <1 kg yr^{-1} from 2013 (as reported to the NPI). The assumed lack of emissions from chlor-alkali production in the global inventories is thus appropriate.

Where specified separately, cremation emissions provide only a small contribution to total intentional use and waste emissions, accounting for 70–170 kg yr^{-1} (1%–12% of the category total). Note that EDGAR appears not to include cremation emissions (Muntean et al., 2014).

The majority of the discrepancy between inventories is therefore driven by assumed waste emissions, which differ by a factor of 100 with much higher values in WHET than in any other inventory (**Table 3**). WHET waste emissions originate from Horowitz et al. (2014). The Horowitz et al. (2014) emissions for 2010 are based on the same mercury consumption data used for AMAP/UNEP (2013), but the inventories differ in their assumptions concerning instantaneous versus delayed release. Although all other inventories assume that mercury emission in a given year is directly related to consumption in that year (i.e., all current consumption directly replaces obsolete products sent to landfill), Horowitz et al. (2014) accounted for delays between consumption and disposal of wiring and industrial measuring devices, with 90% of disposal occurring 30–50 years after consumption. In other words, the Horowitz et al. (2014)/WHET emission estimates for 2010 depend largely on consumption from 1960 to 1980, when mercury supply and use in products was at its peak (Horowitz et al., 2014). This delayed release is an important factor not accounted for in other inventories.

There are large uncertainties in the delayed release implemented by Horowitz et al. (2014) and in the regional distribution of this source used to construct WHET (H Horowitz, personal communication). To regionally distribute the "developed world" (North America, Europe, Oceania) emissions from Horowitz et al. (2014), WHET assumes that the relative fractions of Hg consumption in each region in 2010 can be used to partition both the instantaneous and delayed releases (H Horowitz, personal communication). However, mercury consumption estimates for wiring devices suggest that Oceania represented a much smaller fraction of the total developed world consumption in 1990 than in later years (2.8% in 1990 vs. 6.6% in 2005; Wilson et al., 2010). Earlier consumption data are not available, but assuming consumption scales with GDP (as assumed in Streets et al., 2017) would suggest that Oceania represented an even smaller fraction of the total developed world mercury consumption in the 1960s–1980s. The estimate from WHET therefore likely overestimates the contribution from delayed release in Australia by at least a factor of 2.

There are clearly large uncertainties in the exact amounts and timing of disposal of mercury-containing products in Australia. Although the WHET inventory likely overestimates this source for Australia, this analysis suggests that other inventories assuming only instantaneous release almost certainly underestimate these emissions. The true value likely lies somewhere in between.

3.1.5. Summary and recommendations

Major differences in anthropogenic mercury emission estimates from national and global inventories can largely be explained by a combination of methodological differences and the representative year for which each inventory has been constructed. From analysis of these inventories, we suggest that current Australian anthropogenic emission totals are likely of order 5–10 t yr^{-1} with sectoral contributions of 2–4 t yr^{-1} from fossil fuel combustion, 1–3 t yr^{-1} from metal processing, 1–3 t yr^{-1} from waste, and <1 t yr^{-1} from other industrial sources. Gold production, formerly a dominant source, no longer contributes substantively to Australian mercury emissions.

None of the existing inventories are suitable for use in modeling present-day mercury distributions in Australia. The WHET inventory is particularly problematic as it does not take into account pollution control measures at Australian power plants; however, it is the only inventory to consider the impact of delayed release associated with disposal of mercury-containing products. WHET is also the only inventory to provide multi-decadal (1990–2010) emission estimates calculated using a consistent methodology. This information is critical for evaluating trends in Australian mercury emissions and atmospheric concentrations and for interpreting historical deposition records. However, given the issues identified in WHET, we cannot recommend its use for Australia in its present form.

Alternatively, the Nelson et al. (2012) inventory developed specifically for Australia provides the most robust Australia-specific estimates for most sources. However, this inventory was developed using data for the year 2006 and is therefore nearly 15 years out of date. In the time since, the Gidji gold roaster (Australia's largest mercury emission point source) and Orica chlor-alkali plant have ceased operations, along with a third of Australia's

coal-fired power stations (Burke et al., 2018). These changes are expected to significantly perturb the anthropogenic mercury emissions budget.

We recommend an updated, time-varying anthropogenic mercury emissions inventory be constructed for Australia. Australia's NPI provides annual emission estimates that can be used for this purpose for many source types. There are some exceptions, such as brown coal power stations, which NPI underestimates by an order of magnitude (Nelson, 2007). These can generally be addressed by applying the methods presented in Nelson et al. (2012) and/or AMAP/UNEP (2019) to more recent data. Alternative methods, such as scaling power station mercury emissions to better constrained CO_2 emissions as done by Schofield et al. (n.d.), could also be investigated. For waste, consideration should be given to delayed release, as applied in WHET, but tailored to better account for historical consumption patterns in Australia.

3.2. Biomass burning emissions

Mercury emissions from Australian biomass burning are poorly constrained, with existing estimates providing a wide range from as little as 4 t yr^{-1} to as much as 129 t yr^{-1}. **Figure 3A** shows published estimates of the total Australia-wide emissions of mercury from biomass burning sources, ordered from smallest to largest. The largest two of the six estimates (Packham et al., 2009; Nelson et al., 2012;) are from Australia-specific studies, while the remainder (Friedli et al., 2009; De Simone et al., 2015; Kumar et al., 2018) are from global studies that report the Australian contribution.

Biomass burning emissions from a given vegetation type or biome are typically estimated using a variant of the following equation:

$$E_{\mathrm{Hg}} = \mathrm{EF}_{\mathrm{Hg}} \cdot A \cdot M \cdot C,$$

where E_{Hg} is the emitted mass of mercury, $\mathrm{EF}_{\mathrm{Hg}}$ is the mercury emission factor (mass of mercury emitted per mass of fuel burned), A is the area burned, M is the biomass loading (also known as the fuel loading or biomass density) in mass per area, and C is the combustion completeness (also known as combustion fraction or burning efficiency) representing the fraction of total available fuel that burns. In general, area burned is based on remote-sensing observations from satellite (with notable exceptions discussed below), biomass loading comes from vegetation models, and emission factors are empirically derived.

Figure 3 also shows the estimated area burned (B) and effective emission factors (C) for the six emission estimates provided in (A). Note that biomass loading and combustion completeness are not reported in most studies. The figure shows that much of the variability in mercury emissions can be explained by differences in these two variables, with Packham et al. (2009) notably higher than all other estimates for both parameters.

3.2.1. Burned area

Burned area estimates range from 17 to 146 Mha yr^{-1} with a mean of 59 Mha yr^{-1} and a median of 49 Mha yr^{-1}. Although interannual variability in fire activity can drive

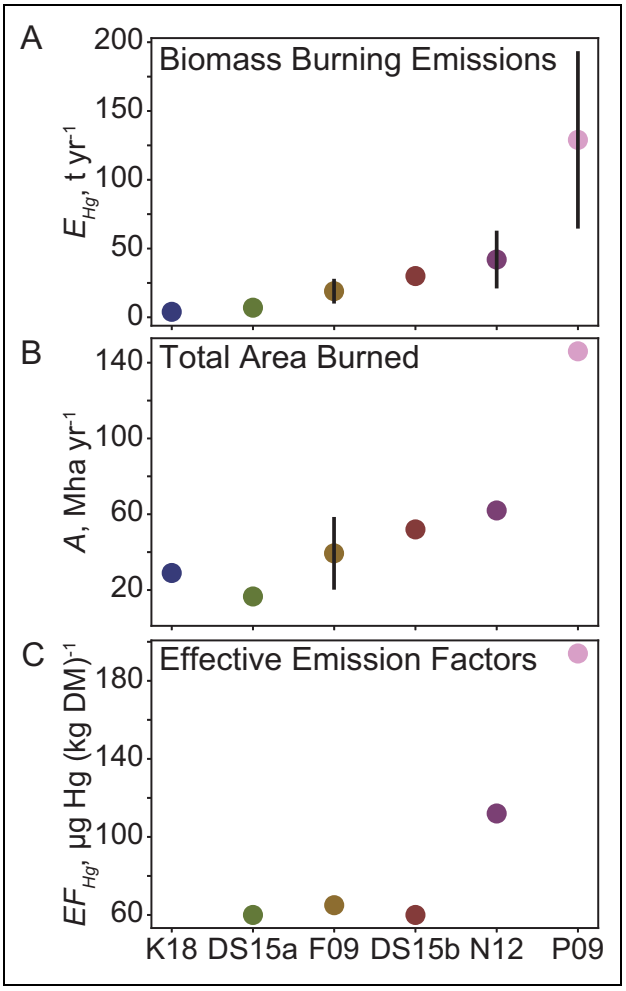

Figure 3. Australian biomass burning emissions and related parameters. Published estimates of (A) mercury emissions from Australian biomass burning (E_{Hg}, t yr^{-1}), along with (B) area burned (A, Mha yr^{-1}) and (C) effective country-wide emission factors ($\mathbf{EF_{Hg}}$, µg Hg (kg fuel) $^{-1}$). Error ranges are included where provided in the original study and shown as black vertical lines (except for K18 in (A), where errors of [+0.8, –0.6] t yr^{-1} are too small to be visible on this scale). Labels on the *x*-axis correspond to the relevant reference: K18 (Kumar et al., 2018), DS15a (De Simone et al., 2015, FINNv1), F09 (Friedli et al., 2009), DS15b (De Simone et al., 2015, GFEDv3), N12 (Nelson et al., 2012), and P09 (Packham et al., 2009). Note that De Simone et al. (2015) do not explicitly provide either area burned or effective emission factors; for these plots, effective emission factors are estimated from their Figure S7, and Australian area burned values for FINNv1 (DS15a) and GFEDv3 (DS15b) are taken from Kumar et al. (2018). DOI: https://doi.org/10.1525/elementa.2020.070.f3

significant variability in a burned area, the estimates in **Figure 3** largely account for this by averaging over periods of at least 5 years. The exception is Nelson et al. (2012), whose estimates are only for the year 2006; however, multiple long-term analyses show 2006 to be a year with average fire activity for Australia (Giglio et al., 2013; Earl and Simmonds, 2017).

Most of the estimates shown in **Figure 3** were derived from satellite data products, including active fires (Nelson et al., 2012; De Simone et al., 2015), fire scars (Nelson et al., 2012), fire radiative power (De Simone et al., 2015), a retrieved burned area product (Friedli et al., 2009; De Simone et al., 2015), or some combination of these. Packham et al. (2009) used a much simpler approach, dividing Australia into 13 fuel types that were each assigned an areal extent (A_i, km^2) and burning frequency (Y_i, yr) derived from Walker (1981). Total area burned was then calculated as $A = \sum_i A_i / Y_i$. The comparison in **Figure 3B** suggests that this simplified method likely overestimates area burned by a factor of 3–8 and as a consequence overestimates total mercury emission (although we cannot quantify the impact because the fires are not evenly distributed across the continent). At the other extreme, the FINNv1 model used by De Simone et al. (2015; DS15a in **Figure 3**) has been shown elsewhere to underestimate burned area in areas where large savanna and grassland fires dominate, including Australia (Shi and Matsunaga, 2017).

3.2.2. Emission factors

The effective emission factors shown in **Figure 3C** represent area-weighted averages over different vegetation types. Note that Nelson et al. (2012) used a single emission factor (112 μg Hg (kg fuel)$^{-1}$) for all Australian ecosystems. Only the Packham et al. (2009) value includes measurements from Australian vegetation; the rest are derived from measurements elsewhere in the world. Although most emission factor estimates are derived from ratios of mercury to other gases measured in atmospheric smoke plumes (e.g., Desservettaz et al., 2017; Howard et al., 2019), the Packham et al. (2009) values instead come from the measured mercury content of biomatter (leaf litter, grass, and bark), assuming all mercury is volatilized during combustion. The latter assumption has not been tested in Australian ecosystems, but based on measurements elsewhere in the world, it could lead to overestimates of 15%–20% (Michelazzo et al., 2010).

Roughly two thirds of the annual burned area in Australia occurs in tropical and subtropical savannas and grasslands (Howard et al., 2019). **Figure 4A** shows the emission factors applied to this ecosystem for the six mercury emission estimates in **Figure 3**, ranging from 17.6 to 212 μg Hg (kg fuel)$^{-1}$. The figure also shows the average emission factor from recent measurements of tropical savanna fire smoke in northern Australia (Desservettaz et al., 2017, D17 in **Figure 4A**). Over four unique smoke events, Desservettaz et al. (2017) found mercury emission factors of 3.45–32.5 μg Hg (kg fuel)$^{-1}$, with an average value of 12.6 ± 11.8 μg Hg (kg fuel)$^{-1}$. These new measurements are significantly lower than the values used previously. Given savanna fires may be responsible for up to 80% of Australian biomass burning emissions (Packham et al., 2009), these new results imply a significant downward revision of the Australian fire emission source. For example, applying the upper limit from Desservettaz et al. (2017) to the tropical savanna eco-regions used in Packham et al. (2009) would bring total Australian biomass burning mercury emissions down from 130 t yr^{-1} to less than 40 t yr^{-1}, even before taking into account the burned area overestimates detailed above.

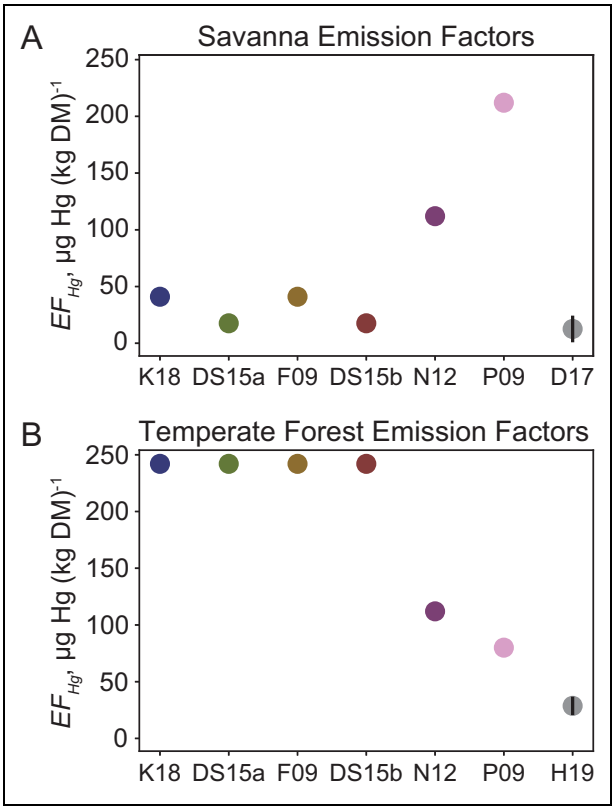

Figure 4. Ecosystem-specific mercury emission factors. Ecosystem-specific estimates of mercury emission factors used to derive the estimates in **Figure 3** for (A) savannas and (B) temperate forests. Abbreviations are explained in **Figure 3**. Also shown are values from recent Australian measurements from Desservettaz et al. (2017; D17 in [A]) and Howard et al. (2019) for temperate forests (H19 in [b]). Only D17 and H19 provide uncertainty estimates, shown as black vertical lines. DOI: https://doi.org/10.1525/elementa.2020.070.f4

Recent measurements also exist for emission factors from Australian temperate forest fires. Using both controlled burns and field sampling, Howard et al. (2019) found temperate fire emission factors of 28.7 ± 8.1 μg Hg (kg fuel)$^{-1}$. As shown in **Figure 4B**, these new measurements are significantly lower than the values used in earlier budget studies, which ranged from 80 to 242 μg Hg (kg fuel)$^{-1}$. Although these ecosystems account for less than 1% of Australia's annual burned area (Howard et al., 2019), these results further imply that prior estimates of Australian fire emissions are likely too high and highlight the need for measurements from Australian ecosystems.

3.2.3. Summary and recommendations

Prior estimates of mercury emissions from Australian fires are likely too high due to errors in assumptions about both area burned and mercury emission factors. Most global and some national estimates have relied on

mercury emission factors derived from non-Australian vegetation fires. New measurements from Australian smoke plumes show that emission factors for both savanna and temperate forest fires are significantly lower than emission factors measured elsewhere in the world. These new measurements also imply much lower emission factors than derived from biomatter measurements of Australian vegetation for reasons that remain unclear. Considering these new measurements, we suggest that Australian biomass burning emission totals are likely of order 5–30 tonnes yr^{-1}.

The analysis presented here shows that the biomass burning source is still highly uncertain, in large part due to a paucity of mercury measurements from Australian vegetation fires. Although tropical and subtropical savanna fires account for roughly two thirds of the area burned in Australia (Howard et al., 2019), the mercury content of smoke from these fires has only been measured in four smoke plumes, all from a single location. Meanwhile, another 30% of Australia's burned area comes from desert and xeric shrubs (Howard et al., 2019), but the mercury content of fire smoke in these ecosystems has never been measured. Measurements of mercury emission factors from diverse Australian vegetation types are sorely needed.

3.3. Soil and vegetation emissions

On the sparsely populated Australian continent, uninhabited landscapes have been predicted to be the dominant source of mercury to the atmosphere. Nelson et al. (2012) found that quasi-natural sources, including both primary emissions from mercury-enriched substrates and reemission of previously deposited anthropogenically sourced mercury, comprise 72% of the total Australian atmospheric mercury budget. Such a large contribution is unique to Australia; globally, quasi-natural emissions (excluding biomass burning) represent roughly a third of the land-based atmospheric source (Selin, 2009).

Despite their prevalence, only one study has attempted to quantify the mercury source from Australian vegetation and soils. Nelson et al. (2012) estimated that these sources emit 148 $\pm$74 t yr^{-1}, with the vast majority (95%) from soils. Nearly all of this source is associated with background or naturally enriched environments; estimated Australia-wide emissions from contaminated soils are only 0.25–0.5 t yr^{-1} (Kocman et al., 2013). The Nelson et al. (2012) estimate was modeled using parameterizations based on known soil characteristics and assumed mercury content in soils, with virtually no Australian observations available as constraints. In the time since, a number of new measurements have been made, which shed further light on the validity of the existing estimate.

3.3.1. Background soils

Few studies have measured the overall fluxes from soils to the atmosphere, and even where these have been measured, the comparison to modeled values is not straightforward. Although models typically parameterize the soil source as a one-way upward flux, air–soil exchange is bidirectional, with upward fluxes from the soil surface countered by downward uptake and deposition processes. Measurements capture the net air-surface exchange rather than the upward flux. The few Australian air-surface flux measurements that exist suggest that net exchange over background sites is near zero: 0.002 $\pm$ 14.2 ng m^{-2} h^{-1} averaged over 14 months at an agricultural grassy site (MacSween et al., 2020), 0.2 $\pm$ 14.5 ng m^{-2} h^{-1} averaged over 3 weeks in austral summer at an alpine grassland (Howard and Edwards, 2018), and 0.36 $\pm$ 0.06 ng m^{-2} h^{-1} over 2 weeks in April (autumn) and June (winter) in northern New South Wales (Edwards and Howard, 2013). In comparison, the (upward) Nelson et al. (2012) modeled mercury fluxes largely fell within 1–4 ng m^{-2} h^{-1} over most of the continent, with occasional values up to 10 ng m^{-2} h^{-1} over dry salt lakes.

A key parameter underlying soil mercury flux estimates is the soil mercury content. To estimate soil mercury content, Nelson et al. (2012) assumed concentrations of 15 ng g^{-1} for sand and sandy soils, 100 ng g^{-1} for peat soils, and 500 ng g^{-1} for saline lakes, with gridded soil type maps used to distribute these spatially. The authors do not provide the resulting landscape-averaged soil mercury concentrations but note typical concentrations of 25 ng g^{-1} in vegetated regions. Given the prevalence of sandy soils across much of the continent (69% on average and up to 100% in nonvegetated regions; Viscarra Rossel et al., 2015), we assume that most Australian soils would fall in the 15–25 ng g^{-1} range in their model.

Recent measurements show significant variability in mercury concentrations in uncontaminated Australian soils. The lowest concentrations were measured in the tropical savanna, where Howard et al. (2017) reported soil mercury of 9.14 $\pm$ 0.58 ng g^{-1} in grassed areas and 26.49 $\pm$ 3.31 ng g^{-1} under forest canopy. In vegetated regions of the southeast, several studies have reported concentrations of 30–70 ng g^{-1}, including from alpine grasslands (48 $\pm$ 9 ng g^{-1}; Howard and Edwards, 2018), agricultural grasslands (69 $\pm$ 22 ng g^{-1}; MacSween et al., 2020), Victorian forests (61.7 $\pm$ 3.6 ng g^{-1} in <212 μm fine soils and 30.1 $\pm$ 1.5 ng g^{-1} in coarse soils; Hellings et al., 2013), and Tasmanian forests (29.4 $\pm$ 17.7 ng g^{-1} and 49.3 $\pm$ 29.0 ng g^{-1} at two nearby sites; Howard et al., 2019). Similar concentrations were also measured at bare soil sites in northern New South Wales (44–65 ng g^{-1}; Edwards and Howard, 2013). Taken together, these measurements suggest that the soil mercury concentrations assumed by Nelson et al. (2012) are reasonable but perhaps on the lower end of expected concentrations in unenriched Australian landscapes, at least in the eastern part of the country.

The magnitude of the soil flux depends not only on soil mercury content but also on environmental variables such as solar and UV-B radiation, air and soil temperatures, soil moisture, and precipitation (Agnan et al., 2015) that modulate the flux. In the absence of Australian data to constrain this relationship, Nelson et al. (2012) parameterized soil mercury fluxes based on soil temperature and under-canopy solar radiation. Short-term Australian measurements have shown that net fluxes correlate much more strongly with air temperature than soil temperature (Edwards and Howard, 2013; Howard and Edwards, 2018).

Solar radiation (but not UV-B radiation) has also been shown to significantly correlate with Australian mercury fluxes, even over bare soils (Edwards and Howard, 2013; Howard and Edwards, 2018).

A recent yearlong study that separately considered upward fluxes provides a more nuanced picture (MacSween et al., 2020). In spring and summer, upward fluxes were significantly correlated with both air and surface soil temperature, with the air temperature correlation stronger than (spring) or equivalent to (summer) the soil temperature correlation. In autumn and winter, however, the correlation with air temperature disappeared (autumn) or weakened (winter), while the correlation with soil temperature reversed to an anticorrelation in autumn and disappeared altogether in winter. Soil volumetric water content also showed a seasonally varying relationship with the upward mercury flux, with positive correlation in spring, summer, and winter and anticorrelation in autumn. Throughout the year, the upward flux was more strongly correlated with solar radiation than with air temperature, soil temperature, or soil water content. As for temperature and water content, the solar radiation correlations were strongest in spring and summer. The authors suggest that the lack of correlation between upward fluxes and environmental variables in autumn and winter may relate to low temperatures and radiation preventing soil mercury photo reduction and subsequent volatilization (MacSween et al., 2020).

3.3.2. Mercury-enriched soils

Parts of Australia are naturally enriched by a large mercury mineral belt along the southeast coast (Rytuba, 2003) along with pockets of high-mercury geogenic deposits (Edwards and Howard, 2013). In addition, a legacy of widespread mining has contaminated Australian soils and vegetation in the vicinity of mining areas (e.g., Abraham et al., 2018a; Schneider et al., 2019). Soils can also be contaminated by deposition from long-running industrial emission sources such as power plants (Martín and Nanos, 2016).

Although Nelson et al. (2012) did not explicitly account for mercury-enriched soils, a few measurements from these environments now exist. Edwards and Howard (2013) sampled a site in inland New South Wales (Pulganbar) with a natural cinnabar deposit that was mined in the early 1900s and found elevated soil mercury concentrations of 250–2300 ng g^{-1} (compared to 44–65 ng g^{-1} at background sites in the same area), with associated net mercury fluxes of 47.2 $\pm$ 3 ng m^{-2} h^{-1}. Similarly, seasonal soil measurements from a legacy mining site in Maldon, Victoria, showed average concentrations of order 2,000–3,000 ng g^{-1} (Abraham et al., 2018b). To the best of our knowledge, no measurements have been made in Australian soils contaminated by power plant emissions, but Schofield et al. (n.d.) show that modeled soil concentrations of up to 1,000 ng g^{-1} and fluxes of 15 ng m^{-2} h^{-1} are needed to match atmospheric observations in Victoria's Latrobe Valley, one of Australia's main power-producing regions.

3.3.3. Summary and recommendations

Although natural environments (soils and vegetation) dominate the Australian landscape, the associated mercury source is very poorly constrained. The only existing estimate suggests a source of 148 $\pm$ 74 t yr^{-1}, primarily from soils (Nelson et al., 2012). Recent measurements suggest that soil mercury concentrations at Australian background sites are generally slightly higher than the values used to derive the existing emission estimate and that the parameterizations used to link soil mercury content to mercury emission should be revisited to account for modulation by air temperature, soil water content, and solar radiation. Mercury emission from contaminated soils (not included in the estimate above) is thought to contribute little to the atmospheric mercury budget (Kocman et al., 2013) but may be regionally important and is worth revisiting given Australia's mining legacy. At this stage, there are insufficient Australian data to quantitatively revise the Nelson et al. (2012) estimate. Increased sampling of mercury emission from diverse Australian landscapes, as well as the relationships between emission, soil mercury content, and environmental drivers, will be necessary to improve soil mercury emission estimates.

4. Deposition of atmospheric mercury to the Australian continent

Mercury is removed from the atmosphere via both wet deposition (scavenging in precipitation) and dry deposition (uptake to surface reservoirs without precipitation). Few observations are available to quantify either process in Australia. Models find dry deposition dominates, responsible for anywhere from two thirds (AMAP/UNEP, 2019) to 90% (Nelson et al., 2009) of the total deposition sink, although there are significant discrepancies in the estimated magnitude of deposition. Here, we summarize model estimates of Australian wet and dry deposition fluxes and new observations that provide some constraints on these processes. We also briefly discuss model estimates of the source attribution of mercury deposited to the Australian continent.

4.1. Wet deposition

Global models generally agree that wet deposition of mercury is lower over Australia than for much of the rest of the world. This is due to a combination of low mercury concentrations in air and limited precipitation over much of the continent. An ensemble of four global models found median wet deposition fluxes of 5 $\pm$ 1 μg m^{-2} yr^{-1} over Australia (AMAP/UNEP, 2019); when scaled by the area of the continent, this would equate to a total wet deposition flux of 30–45 t yr^{-1}. Meanwhile, a continental-scale model found a total flux of only 1.8 t yr^{-1} (Nelson et al., 2009). Clearly, there are large uncertainties in model-based estimates, which require observational constraint.

Although mercury deposition measurement networks have been established across North America (Prestbo and Gay, 2009), Europe (Aas and Bohlin-Nizzetto, 2019), and the Asia-Pacific region (Sheu et al., 2019), deposition measurements for Australia are extremely limited. Wet

deposition data have only been published for three sites, and only one of these has a record spanning more than 8 months. The longest record comes from Cape Grim, a temperate background site in northwest Tasmania, which frequently receives clean air from the Southern Ocean (Crawford et al., 2018). From 3 years of measurements, Sprovieri et al. (2017) report weighted mean wet deposition fluxes of 3.4 μg m^{-2} yr^{-1} with little interannual variability (annual weighted means 3.1–3.8 μg m^{-2} yr^{-1}). The data show strong seasonality driven by rainfall variability, with peak rainfall and deposition fluxes in winter and minima in summer (Sprovieri et al., 2017).

The measured wet deposition fluxes at Cape Grim were on average 5–10 times higher than seen at the three other Southern Hemisphere midlatitude sites with multiyear records (Sprovieri et al., 2017). The other sites included Cape Point, South Africa, which occasionally receives mercury-enriched air transported from African power plants (Bieser et al., 2020), and Amsterdam Island, which receives a similar amount of precipitation as Cape Grim but is more remote. The higher deposition fluxes at Cape Grim may signify that the site is sensitive to local and/or continental mercury. Alternatively, methodological differences may be responsible; Cape Grim was the only site of the four to use a bulk precipitation sampler (Swedish Environmental Research Institute IVL sampler) rather than wet-only collectors (Sprovieri et al., 2017). Bulk samplers can record higher fluxes than wet-only collectors due to the influence of dry deposition (e.g., Morrison et al., 1995), although this difference is not expected to influence measurements in remote areas (Chazin et al., 1995; Landis and Keeler, 1997; Lupo and Stone, 2013), and the GMOS protocols used to harmonize the data should have accounted for any methodological differences (Sprovieri et al., 2017). Nonetheless, it would be useful to test the two sampling methodologies side by side at Cape Grim.

Wet deposition has also been measured at two sites in southeast Australia, one located near Australia's largest coal-fired power plants in the Hunter Valley (New South Wales) and the other in a semi-urban region in northwest Sydney (Dutt et al., 2009). Daily deposition fluxes at the power plant site were roughly twice those at the northwest Sydney site. As at Cape Grim, deposition at both sites was correlated with precipitation. The authors did not report annual mean fluxes as sampling did not cover all months (Dutt et al., 2009), but Nelson et al. (2009) combined the Dutt et al. (2009) volume-weighted mean mercury concentrations in precipitation with monthly mean rainfall data to derive annual fluxes of 3.2 μg m^{-2} yr^{-1} in northwest Sydney and 3.8 μg m^{-2} yr^{-1} near the Hunter Valley power plants. For comparison, the continental-scale model of Nelson et al. (2009) showed wet deposition fluxes of only 1.5 μg m^{-2} yr^{-1} in northwest Sydney and 2.1 μg m^{-2} yr^{-1} at the Hunter Valley site, suggesting a low bias of roughly a factor of 2.

Wet deposition measurements are conspicuously lacking from Australia's tropical north, where rainfall amounts are much higher than in the rest of the country (Sivakumar, 2013). Howard et al. (2017) inferred an important role for wet deposition at the Gunn Point site on Australia's north coast based on an observed wet season drawdown in atmospheric mercury in surface air, but without deposition measurements, they were unable to quantify the associated sink. Measurements made elsewhere in the tropics have shown very high deposition fluxes even in the absence of anthropogenic sources, linked to deep convective scavenging of oxidized mercury from the upper free troposphere (Shanley et al., 2015). Similar processing may be an important factor in the Australian mercury cycle (Shah and Jaeglé, 2017), and deposition measurements in the Australian tropics are sorely needed.

Taken together, the limited Australian wet deposition measurements suggest annual mercury fluxes of 3–4 μg m^{-2} yr^{-1}. There seems to be little difference between annual fluxes at a background site (Cape Grim) and near-source sites (Sydney, Hunter Valley), which could reflect continental influence coupled with higher rainfall amounts at the remote site but could also be due to methodological biases. The data are too limited in spatial and temporal coverage to provide much constraint on model-derived deposition budgets. The Nelson et al. (2009) estimate of a 1.8 t yr^{-1} Australian wet deposition sink may be underestimated somewhat, while the 30–45 t yr^{-1} estimate from global models (with ensemble median fluxes of 2–8 μg m^{-2} yr^{-1}) is likely too high. More observations are needed to verify the model estimates, particularly in the wet tropics.

4.2. Dry deposition and surface uptake

Models agree that dry deposition fluxes are larger than wet deposition fluxes in Australia, but with larger uncertainties. The AMAP/UNEP (2019) ensemble of four global models found median dry deposition fluxes of 10 $\pm$ 5 μg m^{-2} yr^{-1} over Australia. Fluxes simulated by the continental-scale model of Nelson et al. (2009) were generally smaller at 0.5–5 μg m^{-2} yr^{-1} over much of the continent, but with near-source hot spots up to 70 μg m^{-2} yr^{-1}. Summed over the continental scale, these fluxes equate to approximately 35–115 t yr^{-1} from the global models (AMAP/UNEP, 2019) and 21 t yr^{-1} from the continental model (Nelson et al., 2009).

Observational constraints on these simulated deposition fluxes are virtually nonexistent. To our knowledge, dry deposition of reactive mercury (in either gaseous or particle-bound form) has never been measured in Australia. For gaseous elemental mercury, the few observations that exist for Australia are based on measured bidirectional fluxes that represent net surface-air fluxes (e.g., emission minus dry deposition). However, most models (including those cited above) simulate dry deposition as a unidirectional (downward) process (Travnikov et al., 2017) and do not report net fluxes. Although bidirectional parameterizations have been developed (Zhang et al., 2019), these have not yet been implemented in any models reporting Australian mercury fluxes.

As discussed previously, measurements of bidirectional fluxes from Australian background sites show that net elemental mercury exchange is near zero (Edwards and Howard, 2013; Howard and Edwards, 2018; MacSween et al., 2020). All measured sites show consistent diurnal

patterns, with net deposition at night. Mean nighttime net deposition fluxes are small, often not significantly different from zero, with reported values of -1.5 ± 7.8 ng m^{-2} h^{-1} over alpine grasslands (Howard and Edwards, 2018), -0.33 ± 0.05 ng m^{-2} h^{-1} over bare soil (Edwards and Howard, 2013), and -0.22 ± 1.3 ng m^{-2} h^{-1} over agricultural grasslands (MacSween et al., 2020). Nocturnal atmospheric mercury depletion events observed in both tropical (Howard et al., 2017) and temperate (Howard and Edwards, 2018) environments have been linked to dry deposition under stable boundary layers. Howard and Edwards (2018) also found that dry deposition leading to nocturnal depletion events is enhanced in the presence of dew, which they suggest may promote complex surface chemistry driving elemental mercury oxidation to more readily deposited reactive mercury.

Seasonal variability was recently reported for the first time by MacSween et al. (2020), who measured net exchange at a southeastern grassland site over a full annual cycle. They found net deposition in winter (June–July–August), although mean seasonal fluxes were again not significantly different from zero. They attributed the wintertime deposition to stomatal uptake based on simultaneous measurements of CO_2 fluxes showing net uptake to vegetation; unlike in other parts of the world, much of southeastern Australia is sufficiently warm in winter for plant growth to occur (MacSween et al., 2020).

4.3. Sources of mercury deposited to Australia

Global source attribution modeling finds that only a small fraction of the mercury deposited to Australia originates from primary Australian anthropogenic emissions (AMAP/UNEP, 2019), with uncertainties that propagate from the uncertainties in anthropogenic emissions discussed previously. Roughly 80% of total Australian deposition comes from natural and secondary sources (including from Australian surfaces; AMAP/UNEP, 2019). One modeling study found that natural contributions to Australian deposition were dominated by emissions from the ocean (Corbitt et al., 2011); however, there remain major uncertainties in model parameterizations of ocean evasion fluxes, which may impact this result (Horowitz et al., 2017; Zhang et al., 2019). Long-range transport of anthropogenic emissions accounts for the majority of the remaining 20%, with the largest contributions from South America, Africa, and East Asia, in that order (AMAP/UNEP, 2019). Only 6% of the mercury deposition to Australia from primary anthropogenic emissions is attributed to domestic Australian sources (AMAP/UNEP, 2019).

4.4. Summary and recommendations

Deposition of atmospheric mercury is one of the most uncertain parts of the global mercury cycle (Zhang et al., 2019), and these uncertainties are magnified for Australia where deposition measurements are extremely limited. Estimates of total mercury deposition over Australia range from as little as 23 t yr^{-1} (Nelson et al., 2009) to as much as 130 t yr^{-1} (AMAP/UNEP, 2019). The lower end comes from continental-scale modeling, which finds that only 10% of the mercury emitted in Australia is deposited

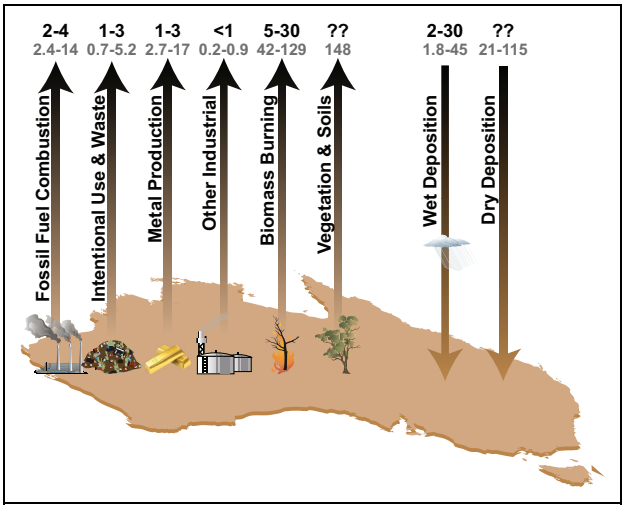

Figure 5. Australian atmospheric mercury budget, in tonnes per year. Black text indicates our best estimates of Australian atmospheric mercury sources and sinks (t yr^{-1}) as described in this work, while gray text shows values compiled from the literature. Question marks indicate that insufficient data exist to make an informed best estimate. Images courtesy of Tracey Saxby, Kim Kraeer, Lucy Van Essen-Fishman, and Diane Kleine via Integration and Application Network, University of Maryland Center for Environmental Science (ian.umces.edu/imagelibrary/). DOI: https://doi.org/10.1525/elementa.2020.070.f5

locally (Nelson et al., 2009); similar estimates have not been provided from global models, which predict significantly higher deposition fluxes (AMAP/UNEP, 2019). However, limited observations of net air-surface exchange suggest that emission and deposition are largely balanced over natural landscapes, at least in the Australian midlatitudes (Edwards and Howard, 2013; Howard and Edwards, 2018; MacSween et al., 2020). At present, it is nearly impossible to validate model estimates of Australian deposition due to both a lack of measurements and simplifications in model parameterization of terrestrial air-surface fluxes. For model validation purposes, we recommend future model studies report net fluxes (e.g., natural emission/reemission minus deposition) alongside gross fluxes to facilitate comparison with observations. New measurements of deposition are urgently required, particularly in the wet tropics, where wet deposition is likely to be a significant mercury sink.

5. Conclusions and future research needs

Figure 5 shows our best estimate of the current sources and sinks of Australian atmospheric mercury. Uncertainty in the total atmospheric source is dominated by natural and legacy emissions from fires, soils, and vegetation. Anthropogenic emissions have decreased over the last two decades following the closures of power plants, chlor-alkali plants, and inefficient gold roasters. Although prior estimates suggest a very large and potentially dominant emission source from background soils, recent air-surface flux observations suggest that this source is likely

balanced by dry deposition and surface uptake at local scales. If so, anthropogenic emissions would still contribute significantly to Australia's overall mercury budget. To improve model estimates of the relative contributions of these sources, an updated Australian anthropogenic mercury emissions inventory and new observationally constrained parameterizations of Australian soil fluxes are needed.

Despite recent efforts, Australia remains one of the most undersampled regions in the world (AMAP/UNEP, 2019). To better constrain the Australian mercury budget and to enable effectiveness evaluation of emission reductions enacted in response to the Minamata Convention, we recommend addressing the following critical future research needs:

1. Continue the ongoing measurements of elemental mercury at the now established coastal background sites at Cape Grim (since 2011) and Gunn Point (since 2014).
2. Restart systematic monitoring of mercury wet deposition at Cape Grim (ended in 2015) and begin mercury wet deposition monitoring at Gunn Point.
3. Establish additional ongoing atmospheric mercury monitoring sites to fill existing data gaps, including at inland sites.
4. Expand capabilities at existing monitoring sites to include measurements of reactive mercury.
5. Undertake measurement campaigns to quantify the mercury emissions released by burning diverse Australian vegetation types, including savannas and desert shrubs.
6. Measure mercury fluxes from Australian soils along with potential environmental correlates.
7. Create an updated, time-varying Australian anthropogenic emissions inventory by combining the most recent estimates from NPI with local understanding of brown coal power station emissions and improved representation of delayed release from disposal of mercury-containing products.
8. Develop parameterizations of mercury emissions from Australian soils, which can be used to drive regional and global atmospheric mercury models.

Australia's role in the global mercury cycle remains highly uncertain. Modeling studies have suggested that the vast majority of the mercury deposited in Australia is emitted elsewhere (Corbitt et al., 2011; Shah and Jaeglé, 2017; AMAP/UNEP, 2019). If these models are correct, Australia stands to benefit significantly from global emission reductions associated with the Minamata Convention. However, existing models have not been evaluated for Australia and show poor ability to reproduce observations at the small handful of other Southern Hemisphere observing sites (Song et al., 2015; Horowitz et al., 2017). The new measurements collected in Australia over the past decade provide an opportunity to evaluate and improve model predictions for Australia and for the Southern Hemisphere more broadly.

Data accessibility statement

No new data were created for this review. All published data are available from the references cited herein. The EDGARv4.tox2 emissions used to calculate the values in Tables 1 and 2 are available from http://edgar.jrc.ec.europa.eu/overview.phpv=4tox2. The AMAP/UNEP (2013) and WHET emissions used to calculate the values in **Table 1** are available from the GEOS-Chem data repository available at Compute Canada: http://geoschemdata.computecanada.ca/ExtData/HEMCO/MERCURY/v2014-09/AMAP/. The underlying sectoral data for WHET used to calculate the values in **Table 2** were provided directly by Y Zhang (personal communication). The NPI emissions data used to create **Figure 2** are available from http://www.npi.gov.au/.

Acknowledgment

We would like to thank Hannah Horowitz, David Streets, and Yanxu Zhang for their help in understanding the inputs used to develop the WHET emission inventory.

Funding

JAF acknowledges funding from the Australian Research Council (DP160101598) and the University of Wollongong Faculty of Science, Medicine and Health. PFN was supported through internal grants from Macquarie University.

Competing interests

JAF has received funding from the Commonwealth Department of Agriculture, Water and the Environment via the National Environmental Science Program and from L'Oréal and UNESCO via a For Women in Science fellowship. PFN has received funding from the Commonwealth Department of Environment, Water, Heritage and the Arts and is co-lead of the UN Environment Partnership on Mercury Control from Coal Combustion.

Author contributions

Contributed to conception and design: JAF, PFN.

Contributed to analysis and interpretation of data: JAF.

Drafted and/or revised the article: JAF, PFN.

Approved the submitted version for publication: JAF, PFN.

References

Aas, W, Bohlin-Nizzetto, P. 2019. Heavy metals and POP measurements, 2017, EMEP/CCC-Report March 2019. Kjeller, Norway: Norwegian Institute for Air Research.

Abraham, J, Dowling, K, Florentine, S. 2018a. Assessment of potentially toxic metal contamination in the soils of a legacy mine site in Central Victoria, Australia. *Chemosphere* **192**: 122–132. DOI: http://dx.doi.org/10.1016/j.chemosphere.2017.10.150.

Abraham, J, Dowling, K, Florentine, S. 2018b. Effects of prescribed fire and post-fire rainfall on mercury mobilization and subsequent contamination assessment in a legacy mine site in Victoria, Australia. *Chemosphere* **190**: 144–153. DOI: http://dx.doi.org/10.1016/j.chemosphere.2017.09.117.

Agnan, Y, Le Dantec, T, Moore, CW, Edwards, GC, Obrist, D. 2015. New constraints on terrestrial surface–atmosphere fluxes of gaseous elemental mercury using a global database. *Environ Sci Technol* **50**(2): 507–524. DOI: http://dx.doi.org/10.1021/acs.est.5b04013.

Amos, HM, Jacob, DJ, Streets, DG, Sunderland, EM. 2013. Legacy impacts of all-time anthropogenic emissions on the global mercury cycle. *Global Biogeochem Cy* **27**(2): 410–421. DOI: http://dx.doi.org/10.1002/gbc.20040.

Arctic Monitoring and Assessment Programme/United Nations Environment Programme. 2008. Technical background report to the Global Atmospheric Mercury Assessment. Arctic Monitoring and Assessment Programme/United Nations Environment Programme Chemicals Branch, pp. 1–159.

Arctic Monitoring and Assessment Programme/United Nations Environment Programme. 2013. Technical background report for the Global Mercury Assessment 2013. Oslo, Norway, pp. 1–271.

Arctic Monitoring and Assessment Programme/United Nations Environment Programme. 2019. Technical background report to the Global Mercury Assessment 2018. Oslo, Norway, pp. 1–430.

Attalla, MI, Malfroy, HR, Morgan, S, Riley, KR, Nelson, PF. 2004. Hazardous pollutants in power station emissions. Research Report 51. Pullenvale, Australia: Cooperative Research Centre for Coal in Sustainable Development.

Bieser, J, Angot, H, Slemr, F, Martin, L. 2020. Atmospheric mercury in the Southern Hemisphere—Part 2: Source apportionment analysis at Cape Point station, South Africa. *Atmospheric Chem Phys* **20**(17): 10427–10439. DOI: http://dx.doi.org/10.5194/acp-20-10427-2020.

Burke, PJ, Best, R, Jotzo, F. 2018. *Closures of coal-fired power stations in Australia: Local unemployment effects*. Acton, Australia: Crawford School of Public Policy, The Australian National University.

Chazin, JD, Allen, MK, Rodger, BC. 1995. Measurement of mercury deposition using passive samplers based on the Swedish (IVL) design. *Atmos Environ* **291**(11): 1201–1209.

Corbitt, ES, Jacob, DJ, Holmes, CD, Streets, DG, Sunderland, EM. 2011. Global source–receptor relationships for mercury deposition under present-day and 2050 emissions scenarios. *Environ Sci Technol* **45**(24): 10477–10484. DOI: http://dx.doi.org/10.1021/es202496y.

Crawford, J, Chambers, SD, Cohen, DD, Williams, AG, Atanacio, A. 2018. Baseline characterisation of source contributions to daily-integrated PM2.5 observations at Cape Grim using Radon-222. *Environ Pollut* **243**(Part A): 37–48. DOI: http://dx.doi.org/10.1016/j.envpol.2018.08.043.

Dale, LS. 2003. Review of trace elements in coal. Project Number C11020. Queensland, Australia: Australian Coal Association Research Program.

Dave, N, Do, T, Palfreyman, D, Feron, PHM. 2011. Impact of post combustion capture of CO2 on existing and new Australian coal-fired power plants. *Energy Procedia* **4**(C): 2005–2019. DOI: http://dx.doi.org/10.1016/j.egypro.2011.02.082.

De Simone, F, Cinnirella, S, Gencarelli, CN, Yang, X, Hedgecock, IM, Pirrone, N. 2015. Model study of global mercury deposition from biomass burning. *Environ Sci Technol* **49**(11): 6712–6721. DOI: http://dx.doi.org/10.1021/acs.est.5b00969.

Desservettaz, M, Paton-Walsh, C, Griffith, DWT, Kettlewell, G, Keywood, MD, Vanderschoot, MV, Ward, J, Mallet, MD, Milic, A, Miljevic, B, Ristovski, ZD, Howard, D, Edwards, GC, Atkinson, B. 2017. Emission factors of trace gases and particles from tropical savanna fires in Australia. *J Geophys Res Atmos* **122**(11): 6059–6074. DOI: http://dx.doi.org/10.1002/2016JD025925.

Dutt, U, Nelson, PF, Morrison, AL, Strezov, V. 2009. Mercury wet deposition and coal-fired power station contributions: an Australian study. *Fuel Process* **90**(11): 1354–1359. DOI: http://dx.doi.org/10.1016/j.fuproc.2009.06.019.

Earl, N, Simmonds, I. 2017. Variability, trends, and drivers of regional fluctuations in Australian fire activity. *J Geophys Res Atmos* **122**(14): 7445–7460.

Edwards, GC, Howard, DA. 2013. Air-surface exchange measurements of gaseous elemental mercury over naturally enriched and background terrestrial landscapes in Australia. *Atmospheric Chem Phys* **13**(10): 5325–5336. DOI: http://dx.doi.org/10.5194/acp-13-5325-2013.

Emmerson, KM, Cope, ME, Hibberd, MF, Torre, P. 2015. Modelling atmospheric mercury from power stations in the Latrobe Valley, Victoria. *Air Quality and Climate Change* **49**(1): 33–37.

Environ. 2006. *Public environmental review: Fimiston gold mine operations extension (Stage 3) and mine closure planning—Appendix F1: Distribution of tellurides and mercury in Fimiston open pit*. Kalgoorlie Consolidated Gold Mines Pty Ltd.

Friedli, HR, Arellano, AF, Cinnirella, S, Pirrone, N. 2009. Initial estimates of mercury emissions to the atmosphere from global biomass burning. *Environ Sci Technol* **43**(10): 3507–3513. DOI: http://dx.doi.org/10.1021/es802703 g.

Giglio, L, Randerson, JT, van der Werf, GR. 2013. Analysis of daily, monthly, and annual burned area using

the fourth-generation global fire emissions database (GFED4). *J Geophys Res Biogeosci* **118**(1): 317–328.

Golev, A, Corder, G. 2016. Modelling metal flows in the Australian economy. *J Clean Prod* **112**: 4296–4303. DOI: http://dx.doi.org/10.1016/j.jclepro.2015.07.083.

Hellings, J, Adeloju, SB, Verheyen, TV. 2013. Rapid determination of ultra-trace concentrations of mercury in plants and soils by cold vapour inductively coupled plasma-optical emission spectrometry. *Microchem J* **111**(C): 62–66. DOI: http://dx.doi.org/10.1016/j.microc.2013.02.007.

Horowitz, HM, Jacob, DJ, Amos, HM, Streets, DG, Sunderland, EM. 2014. Historical mercury releases from commercial products: global environmental implications. *Environ Sci Technol* **48**(17): 10242–10250. DOI: http://dx.doi.org/10.1021/es501337j.

Horowitz, HM, Jacob, DJ, Zhang, Y, Dibble, TS, Slemr, F, Amos, HM, Schmidt, JA, Corbitt, ES, Marais, EA, Sunderland, EM. 2017. A new mechanism for atmospheric mercury redox chemistry: Implications for the global mercury budget. *Atmospheric Chem Phys* **17**(10): 6353–6371. DOI: http://dx.doi.org/10.5194/acp-17-6353-2017.

Howard, D, Edwards, GC. 2018. Mercury fluxes over an Australian alpine grassland and observation of nocturnal atmospheric mercury depletion events. *Atmospheric Chem Phys* **18**(1): 129–142. DOI: http://dx.doi.org/10.5194/acp-18-129-2018.

Howard, D, Macsween, K, Edwards, GC, Desservettaz, M, Guerette, EA, Paton-Walsh, C, Surawski, NC, Sullivan, AL, Weston, C, Volkova, L, Powell, J, Keywood, MD, Reisen, F, Meyer (Mick), CP. 2019. Investigation of mercury emissions from burning of Australian eucalypt forest surface fuels using a combustion wind tunnel and field observations. *Atmos Environ* **202**: 17–27. DOI: http://dx.doi.org/ https://doi.org/10.1016/j.atmosenv.2018.12.015.

Howard, D, Nelson, PF, Edwards, GC, Morrison, AL, Fisher, JA, Ward, J, Harnwell, J, van der Schoot, M, Atkinson, B, Chambers, SD, Griffiths, AD, Werczynski, S, Williams, AG. 2017. Atmospheric mercury in the Southern Hemisphere tropics: Seasonal and diurnal variations and influence of interhemispheric transport. *Atmospheric Chem Phys* **17**(18): 11623–11636. DOI: http://dx.doi.org/10.5194/acp-17-11623-2017.

Kalgoorlie Consolidated Gold Mines Pty Ltd, Ramboll Environ Australia Pty Ltd. 2015. Fimiston Air Quality Management Plan. Available at https://superpit.com.au/wp-content/uploads/2015/01/160617-SER_ENV_PLN1755_KCGM-Fimiston-Air-Quality-Management-Plan-Dec-2015.pdf.

Kocman, D, Horvat, M, Pirrone, N, Cinnirella, S. 2013. Contribution of contaminated sites to the global mercury budget. *Environ Res* **125**(C): 160–170. DOI: http://dx.doi.org/10.1016/j.envres.2012.12.011.

Kumar, A, Wu, S, Huang, Y, Liao, H, Kaplan, JO. 2018. Mercury from wildfires: Global emission inventories and sensitivity to 2000–2050 global change. *Atmos Environ* **173**: 6–15. DOI: http://dx.doi.org/10.1016/j.atmosenv.2017.10.061.

Landis, MS, Keeler, GJ. 1997. Critical evaluation of a modified automatic wet-only precipitation collector for mercury and trace element determinations. *Environ Sci Technol* **31**(9): 2610–2615. DOI: http://dx.doi.org/10.1021/es9700055.

Lupo, CD, Stone, JJ. 2013. Bulk atmospheric mercury fluxes for the Northern Great Plains, USA. *Water Air Soil Pollut* **224**(2): 1582–12. DOI: http://dx.doi.org/10.1007/s11270-013-1437-0.

Lymburner, L, Tan, P, McIntyre, A, Thankappan, M, Sixsmith, J. 2015. *Dynamic land cover dataset version 2.1*. Canberra, Australia: Geoscience Australia.

MacSween, K, Edwards, GC, Beggs, PJ. 2020. Seasonal gaseous elemental mercury fluxes at a terrestrial background site in south-eastern Australia. *Elem Sci Anth* **8**(27): 1–15. DOI: http://dx.doi.org/10.1525/elementa.423.

Mallet, MD, Desservettaz, MJ, Miljevic, B, Milic, A, Ristovski, ZD, Alroe, J, Cravigan, LT, Jayaratne, ER, Paton-Walsh, C, Griffith, DWT, Wilson, SR, Kettlewell, G, van der Schoot, MV, Selleck, P, Reisen, F, Lawson, SJ, Ward, J, Harnwell, J, Cheng, M, Gillett, RW, Molloy, SB, Howard, D, Nelson, PF, Morrison, AL, Edwards, GC, Williams, AG, Chambers, SD, Werczynski, S, Williams, LR, Holly V, Winton, L, Atkinson, B, Wang, X, Keywood, MD. 2017. Biomass burning emissions in north Australia during the early dry season: An overview of the 2014 SAFIRED campaign. *Atmospheric Chem Phys* **17**(22): 13681–13697. DOI: http://dx.doi.org/10.5194/acp-17-13681-2017.

Martín, JAR, Nanos, N. 2016. Soil as an archive of coal-fired power plant mercury deposition. *J Hazard Mat* **308**: 131–138. DOI: http://dx.doi.org/10.1016/j.jhazmat.2016.01.026.

McLagan, DS, Mitchell, CPJ, Steffen, A, Hung, H, Shin, C, Stupple, GW, Olson, ML, Luke, WT, Kelley, P, Howard, D, Edwards, GC, Nelson, PF, Xiao, H, Sheu, G-R, Dreyer, A, Huang, H, Hussain, BA, Lei, YD, Tavshunsky, I, Wania, F. 2018. Global evaluation and calibration of a passive air sampler for gaseous mercury. *Atmospheric Chem Phys* **18**(8): 5905–5919. DOI: http://dx.doi.org/10.5194/acp-18-5905-2018.

Metseo Australia Limited. 2015. Gold mine eliminates processing emissions. Available at https://www.processonline.com.au/content/business/case-study/gold-mine-eliminates-processing-emissions-315587894. Accessed 13 February 2020.

Michelazzo, PAM, Fostier, AH, Magarelli, G, Santos, JC, de Carvalho Jr, JA. 2010. Mercury emissions from forest burning in southern Amazon. *Geophys Res Lett* **37**(9). DOI: http://dx.doi.org/10.1029/2009GL042220.

Morrison, AL, Nelson, PF, Howard, DA. 2015. Ambient atmospheric mercury in the Hunter Valley NSW, in *22nd International Clean Air and Environment Conference*. Melbourne, Australia: 1–6.

Morrison, KA, Kuhn, ES, Watras, CJ. 1995. Comparison of three methods of estimating atmospheric mercury deposition. *Environ Sci Technol* **29**(3): 571–576. DOI: http://dx.doi.org/10.1021/es00003a003.

Muntean, M, Janssens-Maenhout, G, Song, S, Giang, A, Selin, NE, Zhong, H, Zhao, Y, Olivier, JGJ, Guizzardi, D, Crippa, M, Schaaf, E. 2018. Evaluating EDGARv4.tox2 speciated mercury emissions ex-post scenarios and their impacts on modelled global and regional wet deposition patterns. *Atmos Environ* **184**: 56–68. DOI: http://dx.doi.org/10.1016/j.atmosenv.2018.04.017.

Muntean, M, Janssens-Maenhout, G, Song, S, Selin, NE, Olivier, JGJ, Guizzardi, D, Maas, R, Dentener, F. 2014. Trend analysis from 1970 to 2008 and model evaluation of EDGARv4 global gridded anthropogenic mercury emissions. *Sci Total Environ* **494–495**(C): 337–350. DOI: http://dx.doi.org/10.1016/j.scitotenv.2014.06.014.

Nelson, PF. 2007. Atmospheric emissions of mercury from Australian point sources. *Atmos Environ* **41**(8): 1717–1724. DOI: http://dx.doi.org/10.1016/j.atmosenv.2006.10.029.

Nelson, PF, Morrison, AL, Malfroy, HJ, Cope, M, Lee, S, Hibberd, ML, Meyer, CP, McGregor, J. 2012. Atmospheric mercury emissions in Australia from anthropogenic, natural and recycled sources. *Atmos Environ* **62**: 291–302. DOI: http://dx.doi.org/10.1016/j.atmosenv.2012.07.067.

Nelson, PF, Nguyen, H, Morrison, AL, Malfroy, HJ, Cope, ME, Hibberd, MF, Lee, S, McGregor, JL, Meyer (CP), M. 2009. *Mercury sources, transportation and fate in Australia*. Department of Environment, Water, Heritage and the Arts.

Orica. 2014. The Former ChlorAlkali Plant. Available at https://www.orica.com/ArticleDocuments/857/20140205_FCAP_fact_sheet_2.pdf.

Packham, D, Tapper, N, Griepsma, D, Friedli, H, Hellings, J, Harris, S. 2009. Release of mercury in the Australian environment by burning: A preliminary investigation of biomatter and soils. *Air Quality and Climate Change* **43**(1): 1–4.

Page, NC. 2018. Using observations and modelling to quantify mercury biogeochemical cycling in the Australian context [Master's thesis]. Wollongong, Australia: University of Wollongong.

Prestbo, EM, Gay, DA. 2009. Wet deposition of mercury in the U.S. and Canada, 1996–2005: Results and analysis of the NADP mercury deposition network (MDN). *Atmos Environ* **43**(27): 4223–4233. DOI: http://dx.doi.org/10.1016/j.atmosenv.2009.05.028.

Riley, K, Dale, L, Devir, G, Williams, A, Holcombe, D. 2005. Background information for web site on trace elements in coal. Project number C12060. Kenmore, Australia: Australian Coal Association Research Program.

Rytuba, JJ. 2003. Mercury from mineral deposits and potential environmental impact. *Environ Geol* **43**(3): 326–338. DOI: http://dx.doi.org/10.1007/s00254-002-0629-5.

Schneider, L, Allen, K, Walker, M, Morgan, C, Haberle, S. 2019. Using tree rings to track atmospheric mercury pollution in Australia: The legacy of mining in Tasmania. *Environ Sci Technol* **53**(10): 5697–5706. DOI: http://dx.doi.org/10.1021/acs.est.8b06712.

Schofield, R, Utembe, S, Gionfriddo, C, Tate, M, Krabbenhoft, D, et al. n.d. Atmospheric mercury in the La Trobe Valley, Australia: Case study June 2013. *Elementa Science of the Anthropocene*, in press.

Selin, NE. 2009. Global biogeochemical cycling of mercury: A review. *Annu Rev Environ Resour* **34**(1): 43–63. DOI: http://dx.doi.org/10.1146/annurev.environ.051308.084314.

Shah, V, Jaeglé, L. 2017. Subtropical subsidence and surface deposition of oxidized mercury produced in the free troposphere. *Atmospheric Chem Phys* **17**(14): 8999–9017. DOI: http://dx.doi.org/10.5194/acp-17-8999-2017.

Shanley, JB, Engle, MA, Scholl, M, Krabbenhoft, DP, Brunette, R, Olson, ML, Conroy, ME. 2015. High mercury wet deposition at a "clean air" site in Puerto Rico. *Environ Sci Technol* **49**(20): 12474–12482. DOI: http://dx.doi.org/10.1021/acs.est.5b02430.

Sheu, G, Gay, D, Schmeltz, D, Olson, M, Chang, S-C, Lin, D-W, Nguyen, L. 2019. A new monitoring effort for Asia: The Asia Pacific Mercury Monitoring Network (APMMN). *Atmosphere* **10**(9): 481–17. DOI: http://dx.doi.org/10.3390/atmos10090481.

Shi, Y, Matsunaga, T. 2017. Temporal comparison of global inventories of CO2 emissions from biomass burning during 2002–2011 derived from remotely sensed data. *Environ Sci Pollut Res* **24**(20): 1–12. DOI: http://dx.doi.org/10.1007/s11356-017-9141-z.

Sinclair, D, Schneider, L. 2019. Mercury emissions, regulation and governance of coal-fired power stations in Victoria, Australia. *Environ Plan Law J* **36**: 630–641.

Sivakumar, B. 2013. Water resources and environment in Australia. *Stoch Environ Res Risk Assess* **28**(1): 1–2. DOI: http://dx.doi.org/10.1007/s00477-013-0785-z.

Slemr, F, Angot, H, Dommergue, A, Magand, O, Barret, M, Weigelt, A, Ebinghaus, R, Brunke, E-G, Pfaffhuber, KA, Edwards, G, Howard, D, Powell, J, Keywood, M, Wang, F. 2015. Comparison of mercury concentrations measured at several sites in the Southern Hemisphere. *Atmospheric Chem Phys* **15**(6): 3125–3133. DOI: http://dx.doi.org/10.5194/acp-15-3125-2015.

Song, S, Selin, NE, Soerensen, AL, Angot, H, Artz, R, Brooks, S, Brunke, E-G, Conley, G, Dommergue, A, Ebinghaus, R, Holsen, TM, Jaffe, DA, Kang, S, Kelley, P, Luke, WT, Magand, O, Marumoto, K, Pfaffhuber, KA, Ren, X, Sheu, G-R, Slemr, F, Warneke, T, Weigelt, A, Weiss-Penzias, P, Wip, DC, Zhang, Q. 2015. Top-down constraints on atmospheric mercury emissions and implications for global biogeochemical cycling. *Atmospheric Chem*

Phys **15**(12): 7103–7125. DOI: http://dx.doi.org/10.5194/acp-15-7103-2015.

Sprovieri, F, Pirrone, N, Bencardino, M, D'Amore, F, Angot, H, Barbante, C, Brunke, E-G, Arcega-Cabrera, F, Cairns, W, Comero, S, Diéguez, MC, Dommergue, A, Ebinghaus, R, Feng, XB, Fu, X, Garcia, PE, Gawlik, BM, Hageström, U, Hansson, K, Horvat, M, Kotnik, J, Labuschagne, C, Magand, O, Martin, L, Mashyanov, N, Mkololo, T, Munthe, J, Obolkin, V, Islas, MR, Sena, F, Somerset, V, Spandow, P, Vardè, M, Walters, C, Wängberg, I, Weigelt, A, Yang, X, Zhang, H. 2017. Five-year records of mercury wet deposition flux at GMOS sites in the Northern and Southern hemispheres. *Atmospheric Chem Phys* **17**(4): 2689–2708. DOI: http://dx.doi.org/10.5194/acp-17-2689-2017.

Streets, DG, Devane, MK, Lu, Z, Bond, TC, Sunderland, EM, Jacob, DJ. 2011. All-time releases of mercury to the atmosphere from human activities. *Environ Sci Technol* **45**(24): 10485–10491. DOI: http://dx.doi.org/10.1021/es202765 m.

Streets, DG, Horowitz, HM, Jacob, DJ, Lu, Z, Levin, L, ter Schure, AFH, Sunderland, EM. 2017. Total mercury released to the environment by human activities. *Environ Sci Technol* **51**(11): 5969–5977. DOI: http://dx.doi.org/10.1021/acs.est.7b00451.

Streets, DG, Horowitz, HM, Lu, Z, Levin, L, Thackray, CP, Sunderland, EM. 2019. Global and regional trends in mercury emissions and concentrations, 2010–2015. *Atmos Environ* **201**: 417–427. DOI: http://dx.doi.org/10.1016/j.atmosenv.2018.12.031.

Travnikov, O, Angot, H, Artaxo, P, Bencardino, M, Bieser, J, D'Amore, F, Dastoor, A, De Simone, F, Diéguez, MC, Dommergue, A, Ebinghaus, R, Feng, XB, Gencarelli, CN, Hedgecock, IM, Magand, O, Martin, L, Matthias, V, Mashyanov, N, Pirrone, N, Ramachandran, R, Read, KA, Ryjkov, A, Selin, NE, Sena, F, Song, S, Sprovieri, F, Wip, D, Wängberg, I, Yang, X. 2017. Multi-model study of mercury dispersion in the atmosphere: atmospheric processes and model evaluation. *Atmospheric Chem Phys* **17**(8): 5271–5295. DOI: http://dx.doi.org/10.5194/acp-17-5271-2017.

Viscarra Rossel, RA, Chen, C, Grundy, MJ, Searle, R, Clifford, D, Campbell, PH. 2015. The Australian three-dimensional soil grid: Australia's contribution to the GlobalSoilMap project. *Soil Research* **53**(8): 845–20. DOI: http://dx.doi.org/10.1071/SR14366.

Walker, J. 1981. Fuel dynamics in Australian vegetation, in Gill, AM, Groves, RH, Noble, IR, eds., *Fire and the Australian Biota*. Canberra, Australia: Australian Academy of Sciences: 101–127.

Wilson, S, Munthe, J, Sundseth, K, Kindbom, K, Maxson, P, Pacyna, J, Steenhuisen, F. 2010. Updating historical global inventories of anthropogenic mercury emissions to air. Oslo, Norway: Arctic Monitoring and Assessment Programme (AMAP). AMAP Technical Report No.: 3.

Zhang, L, Zhou, P, Cao, S, Zhao, Y. 2019. Atmospheric mercury deposition over the land surfaces and the associated uncertainties in observations and simulations: A critical review. *Atmospheric Chem Phys* **19**(24): 15587–15608. DOI: http://dx.doi.org/10.5194/acp-19-15587-2019.

Zhang, Y, Horowitz, H, Wang, J, Xie, Z, Kuss, J, Soerensen, AL. 2019. A coupled global atmosphere-ocean model for air-sea exchange of mercury: Insights into wet deposition and atmospheric redox chemistry. *Environ Sci Technol* **53**(9): 5052–5061.

Zhang, Y, Jacob, DJ, Horowitz, HM, Chen, L, Amos, HM, Krabbenhoft, DP, Slemr, F, St. Louis, VL, Sunderland, EM. 2016. Observed decrease in atmospheric mercury explained by global decline in anthropogenic emissions. *PNAS* **113**(3): 526–531. DOI: http://dx.doi.org/10.1073/pnas.1516312113.

How to cite this article: Fisherm, JA, Nelson, PF. 2020. Atmospheric mercury in Australia: Recent findings and future research needs. *Elem Sci Anth*. 8: 1. DOI: https://doi.org/10.1525/elementa.2020.070.

Domain Editor-in-Chief: Detlev Helmig, Boulder A.I.R. LLC, Boulder, CO, USA.

Guest Associate Editor: Alexandra Steffen, Environment and Climate Change Canada, Toronto, Canada.

Knowledge Domain: Atmospheric Science

Part of an Elementa Forum: Mercury in the Southern Hemisphere and Tropics

Published: December 23, 2020 **Accepted:** October 17, 2020 **Submitted:** June 14, 2020

ELEMENTA Science of the Anthropocene

Elem Sci Anth is a peer-reviewed open access journal published by University of California Press.

OPEN ACCESS